



BACHELOR'S THESIS

---

CONTRIBUTION TO THE ANOMALOUS MAGNETIC  
MOMENT OF THE MUON IN SCALAR AND FERMION  
EXTENDED MODELS

---

Submitted by

**Julius Altebockwinkel**

First examiner

Dr. Vishnu Padmanabhan Kovilakam

Second examiner

Prof. Dr. Michael Klasen

University of Münster  
Intitute for Theoretical Physics

## Abstract

The anomalous magnetic moment of the muon (AMM),  $a_\mu = (g_\mu - 2)/2$ , presently stands among the most important probes for physics beyond the Standard Model. This thesis investigates contributions to  $a_\mu$  arising from extended scalar and fermion sectors introduced by the Two-Higgs-doublet model and couplings between the distinct lepton generations. We present a compact review of the Standard Model prediction, highlighting the role of QED in the computation of loop contributions to the AMM and then derive general one-loop correction formulae, involving scalars and fermions, relevant for the model studied. Using analytic expressions and numerical scans of the parameter space, we compare model predictions to the measurement of  $a_\mu$  and to experimentally found constraints in the parameter space. The results identify regions where scalar-mediated contributions can reduce the tension between theory and experiment. Overall, the work clarifies how simple scalar and fermion extensions can (partially) address the muon  $g - 2$  discrepancy and maps the most promising targets for experimental scrutiny in the near future.

# Contents

<b>1</b>	<b>Introduction</b>	<b>1</b>
<b>2</b>	<b>Description of the Magnetic Moment within the Standard Model</b>	<b>3</b>
2.1	Non-relativistic limit of the Dirac Equation . . . . .	3
2.2	Extraction of QED form factors . . . . .	7
2.3	One-Loop Contribution within Quantum Electrodynamics . . . . .	9
<b>3</b>	<b>One-Loop Contributions from Scalar-Fermion Interactions</b>	<b>14</b>
3.1	Interaction of a charged fermion with the EM field . . . . .	15
3.2	Interaction of a charged scalar with the EM field . . . . .	19
<b>4</b>	<b>Contributions within the Two-Higgs-Doublet model</b>	<b>21</b>
4.1	Introduction to the Two-Higgs-Doublet Model . . . . .	21
4.2	Analysis of the Impact on muon $g-2$ by different Yukawa Coupling textures .	23
4.2.1	Texture 1: Muon-Muon Coupling . . . . .	24
4.2.2	Texture 2 & 3: Tauon-Muon and Electron-Muon Coupling . . . . .	27
4.2.3	Texture 4: Muon - Tauon / Tauon - Muon Coupling . . . . .	29
4.2.4	Comparison of Parameter spaces from the distinct textures . . . . .	31
<b>5</b>	<b>Conclusion</b>	<b>33</b>
	<b>Appendix</b>	<b>34</b>
A.1	Gamma matrices: Formulas and identities . . . . .	34
A.2	Gordon decomposition . . . . .	34
A.3	Feynman rules . . . . .	35
A.4	Feynman-Parameterization . . . . .	36
A.5	Contribution to the AMM by the Internal Scalar-Photon interaction . . . . .	36
A.6	Mass Matrix Scalar Bosons . . . . .	38
A.7	Projection operators . . . . .	40
	<b>References</b>	<b>41</b>

# 1 Introduction

The Standard Model (SM) of particle physics is declared to be one of the most remarkable achievements of modern science. Developed throughout the second half of the 20th century, it successfully unified the electromagnetic, weak, and strong interactions in a consistent quantum field theory and provides an appropriate description of the observed quarks, leptons and gauge bosons. The prediction and successful experimental discovery of the charm quark, the  $W$  and  $Z$  bosons, the gluon and the Higgs boson prove the comprehensive correctness of the SM. Despite these successes, the SM seems to be incomplete: it does not include gravity, it does not offer a suitable candidate for dark matter and it does not explain the baryon asymmetry of the universe. These conceptual and empirical shortcomings imply that the SM is likely an effective theory valid up to some scale but motivate the search for physics beyond the Standard Model (BSM) [1].

A particularly sensitive probe of physics BSM is the anomalous magnetic moment of the muon (AMM),  $a_\mu = (g_\mu - 2)/2$ , which describes the discrepancy between the experimentally measured value of the magnetic moment of the muon and the relativistically predicted value  $g_\mu = 2$ . The latter results from the relativistic version of the Schrödinger equation, namely the Dirac equation and was found by Paul Dirac in the first half of the 20th century. The SM provides a powerful mathematical framework, called quantum electrodynamics, in which quantum loop effects induce small corrections to the so called Landé-factor  $g_\mu = 2$ . The first-order QED correction was computed 1949 by Julian Schwinger [2],

$$a_\mu^{(1),\text{QED}} = \frac{\alpha}{2\pi},$$

and subsequent higher-order QED, electroweak and hadronic contributions have been computed to obtain the total SM predicted value [3]

$$a_\mu^{\text{SM}} = 116591810(43) \cdot 10^{-11}.$$

The Muon  $g - 2$  Collaboration has published the latest international world average for the experimental value of  $g - 2$  in June, 2025 [4]:

$$a_\mu^{\text{exp}} = 1165920715(145) \cdot 10^{-12}$$

Therefore, the total discrepancy between theory and experiment reaches an all-time high of

$$\Delta a_\mu = a_\mu^{\text{exp}} - a_\mu^{\text{SM}} = (2.61 \pm 0.15) \cdot 10^{-9}$$

The exceptional precision of both theoretical calculations and experimental measurements makes  $a_\mu$  the most important hint for physics BSM.

The aim of this thesis is to investigate whether scalar extensions of the SM can account for the observed anomaly in  $a_\mu$ . Concretely, we derive and evaluate one-loop contributions to the muon electromagnetic vertex arising from internal charged scalars and fermions and apply these results to the Two-Higgs-Doublet Model (2HDM). We study representative Yukawa textures and scan the dependence of the scalar-induced contribution on masses and couplings, identifying parameter regions capable of producing corrections to  $a_\mu$  of the required magnitude while respecting experimental constraints on these parameter spaces.

---

The outline of the thesis is given as follows. Chapter 2 derives  $g = 2$  from the Dirac equation and reproduces Schwinger's leading QED correction  $a = \alpha/2\pi$  via an explicit one-loop calculation. This chapter also fixes the form-factor conventions used throughout and does thus provide the mathematical description of the AMM within the SM. Chapter 3 derives general one-loop integrals for diagrams with an internal charged scalar and fermion coupled to the electromagnetic field. The results are presented as Feynman-parameterized integrals and compact analytic expressions suitable for numerical evaluation. Chapter 4 applies the formulae from Chapter 3 to the 2HDM. After a brief model introduction we compute scalar contributions to  $a_\mu$  for several Yukawa coupling textures and discuss how scalar masses and coupling choices affect the sign and magnitude of the contribution. Finally, we summarize the results and discuss implications for future experimental and theoretical work.

## 2 Description of the Magnetic Moment within the Standard Model

The magnetic moment of a charged particle encapsulates its response to an external magnetic field and serves as a window into both its internal structure and the underlying dynamics dictated by quantum field theory. In non-relativistic electrodynamics, one can derive the familiar relation between angular momentum and magnetic dipole moment by modeling a point particle of charge  $q$  and mass  $m$  moving on a circular orbit of radius  $r$ . Identifying the current  $I = q/T$  with the orbital period  $T = 2\pi r/v$  and the orbital angular momentum  $\mathbf{L} = m \mathbf{r} \times \mathbf{v}$ , one finds

$$\boldsymbol{\mu}_{\text{orb}} = I A \hat{\mathbf{n}} = \frac{q}{2m} \mathbf{L}, \quad (2.0.1)$$

where  $A = \pi r^2$  and  $\hat{\mathbf{n}}$  is the unit vector normal to the orbital plane. This result is only valid for a purely orbital angular momentum though. However, quantum mechanics introduces another “intrinsic” angular momentum for particles, called spin. Paul Dirac firstly derived a relativistic Lorentz invariant version of the Schrödinger equation that simultaneously described spin-affected particles. This so-called Dirac equation shows that the contribution to the magnetic moment of a particle by its spin is double the contribution by its orbital angular momentum. In the following, it is first shown that the Pauli Equation is the non-relativistic limit of the Dirac equation and second the so-called *Landé-factor*  $g = 2$  is derived via the Dirac equation.

### 2.1 Non-relativistic limit of the Dirac Equation

The Schrödinger equation was one of the most powerful equations set up in the early 20th century, giving quantum mechanics a tool to derive quantitative explanations for many observations measured on quantum scales. Till date, the Schrödinger equation is taught throughout the fundamental lectures on quantum theory. Analogously to the Hamilton function in classical dynamics, the Hamilton operator  $\hat{H}$  describes the evolution of a quantum state  $\Psi$  in the following way:

$$\hat{H}\Psi = i \frac{\partial}{\partial t} \Psi = \left( \frac{\hat{\mathbf{p}}^2}{2m} + \hat{V}(\mathbf{x}, t) \right) \Psi \quad (2.1.1)$$

Unfortunately, the Schrödinger equation is not Lorentz invariant and thus not valid for relativistic velocities and energies, which occur in experiments exploring properties of elementary particles. From this point forward, natural units are used, meaning  $\hbar = c = 1$ . The following considerations are based on [5] (p. 74ff., 100ff.)

It seems natural to begin with the relativistic Energy-momentum relation

$$E^2 = m^2 + \mathbf{p}^2 \quad (2.1.2)$$

to derive a Lorentz invariant version of the Schrödinger equation. If we insert the operator substitutions

$$E \rightarrow i \frac{\partial}{\partial t} \quad \text{and} \quad \mathbf{p} = -i \nabla \quad (2.1.3)$$

we obtain the *Klein-Gordon-equation* (KGE)

$$\left( \square^2 + m^2 \right) \Psi = 0, \quad (2.1.4)$$

where the contravariant generalization of (2.1.3)

$$p^\mu = i\partial^\mu \quad \text{with} \quad \partial^\mu = \left( \frac{\partial}{\partial t}, -\nabla \right) \quad (2.1.5)$$

was used to define the D'Alembert operator

$$\square^2 \equiv \partial_\mu \partial^\mu = \left( \frac{\partial^2}{\partial t^2} - \nabla^2 \right). \quad (2.1.6)$$

Although equation (2.1.4) satisfies Lorentz invariance, it still comes with two disadvantages that can not be neglected. First, unlike the Schrödinger equation, the KGE contains second order time derivatives, which implies the necessity of two initial conditions instead of one. Second, the KGE only holds for spinless particles and thus cannot describe fermions with spin- $\frac{1}{2}$ .

To solve the first problem, Paul Dirac achieved to develop a linearized version of the KGE via the ansatz

$$\hat{H} |\psi\rangle = (\boldsymbol{\alpha} \cdot \mathbf{p} + \beta m) |\psi\rangle, \quad (2.1.7)$$

where  $\alpha$  and  $\beta$  are unknown structures that are to satisfy the conditions

$$\{\alpha_i, \alpha_j\} = 2\delta_{ij}, \quad \{\alpha_i, \beta\} = 0, \quad \beta^2 = \mathbb{1} \quad (2.1.8)$$

in order to fulfill relativistic Energy-momentum relation (2.1.2):

$$\begin{aligned} \hat{H}^2 |\psi\rangle &= (\alpha_i p_i + \beta m) (\alpha_j p_j + \beta m) |\psi\rangle \\ &= \left( \underbrace{\alpha_i^2}_{\stackrel{!}{=}\mathbb{1}} p_i^2 + \underbrace{(\alpha_i \alpha_j + \alpha_j \alpha_i)}_{\stackrel{!}{=}0} p_i p_j + \underbrace{(\alpha_i \beta + \beta \alpha_i)}_{\stackrel{!}{=}0} p_i m + \underbrace{\beta^2}_{\stackrel{!}{=}\mathbb{1}} m^2 \right) |\psi\rangle \end{aligned} \quad (2.1.9)$$

It turns out that the structures needed to fulfill the properties (2.1.8) are the *Dirac-matrices*

$$\boldsymbol{\gamma} = (\beta, \beta \boldsymbol{\alpha}), \quad (2.1.10)$$

for which will use the so-called Dirac representation

$$\boldsymbol{\alpha} = \begin{pmatrix} 0 & \boldsymbol{\sigma} \\ \boldsymbol{\sigma} & 0 \end{pmatrix} \quad \text{and} \quad \beta = \begin{pmatrix} \mathbb{1} & 0 \\ 0 & -\mathbb{1} \end{pmatrix}, \quad (2.1.11)$$

where  $\boldsymbol{\sigma}$  represents the Pauli matrices

$$\sigma_1 = \begin{pmatrix} 0 & 1 \\ 1 & 0 \end{pmatrix}, \quad \sigma_2 = \begin{pmatrix} 0 & -i \\ i & 0 \end{pmatrix}, \quad \sigma_3 = \begin{pmatrix} 1 & 0 \\ 0 & -1 \end{pmatrix}. \quad (2.1.12)$$

Since  $\boldsymbol{\alpha}$  and  $\beta$  are  $4 \times 4$  matrices,  $|\psi\rangle$  must be a four component vector, namely a *Dirac spinor*, which can be expressed as a linear combination

$$|\psi\rangle = \begin{pmatrix} \psi_A \\ 0 \end{pmatrix} + \begin{pmatrix} 0 \\ \psi_B \end{pmatrix}, \quad \text{where} \quad \psi_A = \begin{pmatrix} \psi_1 \\ \psi_2 \end{pmatrix} \quad \text{and} \quad \psi_B = \begin{pmatrix} \psi_3 \\ \psi_4 \end{pmatrix}. \quad (2.1.13)$$

Multiplying the ansatz (2.1.7) with  $\beta$  from the left leads to

$$i\beta \frac{\partial}{\partial t} |\psi\rangle = (-i\beta \boldsymbol{\alpha} \nabla + m) |\psi\rangle, \quad (2.1.14)$$

from which we obtain the covariant *Dirac equation* in coordinate representation<sup>1</sup>

$$(i\gamma^\mu \partial_\mu - m) |\psi\rangle \equiv (i\rlap{\not{\partial}} - m) |\psi\rangle = 0 \quad (2.1.15)$$

or equivalently in momentum representation

$$(\rlap{\not{p}} - m) |\psi\rangle = 0. \quad (2.1.16)$$

Now, that the structure and form of the Dirac equation for a free particle has been revealed, the next step will be to consider the effect of the contravariant electromagnetic field  $A^\mu = (\Phi, \mathbf{A})$ , with the electric scalar potential  $\Phi$  and the magnetic vector potential  $\mathbf{A}$ . In the presence of an EM field, the Hamiltonian becomes

$$\hat{H}^{\text{EM}} = \boldsymbol{\alpha} (\mathbf{p} + e\mathbf{A}) + \beta m - e\Phi. \quad (2.1.17)$$

which transforms the Dirac equation within the Dirac representation into

$$\hat{H}^{\text{EM}} |\psi\rangle = \begin{pmatrix} m - e\Phi & \boldsymbol{\sigma} (\mathbf{p} + e\mathbf{A}) \\ \boldsymbol{\sigma} (\mathbf{p} + e\mathbf{A}) & -(m + e\Phi) \end{pmatrix} \begin{pmatrix} \psi_A \\ \psi_B \end{pmatrix} = E |\psi\rangle. \quad (2.1.18)$$

Eq. (2.1.18) can be split up into a set consisting of two coupled two-component equations:

$$\begin{cases} (E - m + e\Phi) \psi_A = \boldsymbol{\sigma} (\mathbf{p} + e\mathbf{A}) \psi_B & \text{(I)} \\ (E + m + e\Phi) \psi_B = \boldsymbol{\sigma} (\mathbf{p} + e\mathbf{A}) \psi_A & \text{(II)} \end{cases} \quad (2.1.19)$$

Multiplying (II) with  $(E + m + e\Phi)^{-1} \boldsymbol{\sigma} (\mathbf{p} + e\mathbf{A})$  and inserting it into (I) yields

$$\frac{(\boldsymbol{\sigma} (\mathbf{p} + e\mathbf{A}))^2}{E + m + e\Phi} \psi_A = (E - m + e\Phi) \psi_A \quad (2.1.20)$$

In the non-relativistic limit we can approximate  $E \approx m$  and  $m \gg e\Phi$ , which we can use to simplify (2.1.20) to

$$(E - m + e\Phi) \psi_A \approx \frac{1}{2m} (\underbrace{\boldsymbol{\sigma} (\mathbf{p} + e\mathbf{A})}_{\equiv \mathbf{p}'})^2 \psi_A \quad (2.1.21)$$

To obtain the non-relativistic Schrödinger equation, we need to simplify the right hand side of (2.1.21). This is done by recalling that the Pauli matrices anticommute

$$\{\sigma^i, \sigma^j\} = 2\delta^{ij} \quad (2.1.22)$$

and that the product of two Pauli matrices satisfies

$$\sigma^i \sigma^j = \delta^{ij} + i\varepsilon^{ijk} \sigma^k. \quad (2.1.23)$$

Hence, we can rewrite (2.1.21) as

$$\frac{1}{2m} (\sigma^i p_i)^2 \psi_A \stackrel{(2.1.22)}{=} \frac{1}{2m} \left( p_i^2 + \sigma^1 \sigma^2 (p_1 p_2' - p_2 p_1') + \sigma^2 \sigma^3 (p_2 p_3' - p_3 p_2') + \sigma^3 \sigma^1 (p_3 p_1' - p_1 p_3') \right) \psi_A. \quad (2.1.24)$$

Plugging in  $\mathbf{p}'$  and using (2.1.23) leads to

$$\begin{aligned} \frac{1}{2m} (\sigma^i p_i')^2 \psi_A &\stackrel{(2.1.23)}{=} \frac{1}{2m} \left\{ p_i'^2 + i \left[ \sigma^3 \left( (i\partial_1 + eA_1)(i\partial_2 + eA_2) - (i\partial_2 + eA_2)(i\partial_1 + eA_1) \right) \right. \right. \\ &\quad \left. \left. + \sigma^1 \left( (i\partial_2 + eA_2)(i\partial_3 + eA_3) - (i\partial_3 + eA_3)(i\partial_2 + eA_2) \right) \right] \right\} \psi_A \end{aligned}$$

<sup>1</sup> The Dirac adjoint of this equation is given as  $\langle \bar{\psi} | (\rlap{\not{p}} + m) = 0$ .

$$\begin{aligned}
 & +\sigma^2\left((i\partial_3 + eA_3)(i\partial_1 + eA_1) - (i\partial_1 + eA_1)(i\partial_3 + eA_3)\right)\psi_A \\
 = & \frac{1}{2m}\left\{p_i'^2 - e\left[\sigma^3\left(\partial_1 A_2 + A_1\partial_2 - \partial_2 A_1 - A_2\partial_1\right)\right.\right. \\
 & \left.+\sigma^1\left(\partial_2 A_3 + A_2\partial_3 - \partial_3 A_2 - A_3\partial_2\right)\right. \\
 & \left.+\sigma^2\left(\partial_3 A_1 + A_3\partial_1 - \partial_1 A_3 - A_1\partial_3\right)\right\}\psi_A, \tag{2.1.25}
 \end{aligned}$$

where Schwarz' theorem was used in the second step. Next, the product rule leads to

$$\begin{aligned}
 \frac{1}{2m}(\sigma^i p_i')^2 &= \frac{1}{2m}\left\{p_i'^2 - e\left[\sigma^3\left((\partial_1 A_2)\psi_A + \underline{A_2}(\partial_1\psi_A) + \underline{A_1}(\partial_2\psi_A) - (\partial_2 A_1)\psi_A\right.\right.\right. \\
 & \left. - \underline{A_1}(\partial_2\psi_A) - \underline{A_2}(\partial_1\psi_A)\right) + \sigma^1\left((\partial_2 A_3)\psi_A\right. \\
 & \left. + \underline{A_3}(\partial_2\psi_A) + \underline{A_2}(\partial_3\psi_A) - (\partial_3 A_2)\psi_A - \underline{A_2}(\partial_3\psi_A)\right. \\
 & \left. - \underline{A_3}(\partial_2\psi_A)\right) + \sigma^2\left((\partial_3 A_1)\psi_A + \underline{A_1}(\partial_3\psi_A) + \underline{A_3}(\partial_1\psi_A)\right. \\
 & \left. - (\partial_1 A_3)\psi_A - \underline{A_3}(\partial_1\psi_A) - \underline{A_1}(\partial_3\psi_A)\right)\left.\right\} \\
 &= \frac{1}{2m}\left(\mathbf{p}'^2 - e\sigma^k \varepsilon_{ijk}\partial_i A_j\right)\psi_A \\
 &= \left(\frac{1}{2m}(\mathbf{p} + e\mathbf{A})^2 + \frac{e}{2m}\boldsymbol{\sigma} \cdot \mathbf{B}\right)\psi_A \tag{2.1.26}
 \end{aligned}$$

Comparing with eq. (2.1.21) and using the spin operator  $\mathbf{S}$  to be  $\mathbf{S} = \boldsymbol{\sigma}/2$  gives the well-known Schrödinger equation for a spin- $\frac{1}{2}$  particle in an electromagnetic field

$$\hat{H}_S^{\text{EM}}\psi_A = \left(\frac{1}{2m}(\mathbf{p} + e\mathbf{A})^2 + 2\frac{e}{2m}\mathbf{S}\mathbf{B} - e\Phi\right)\psi_A. \tag{2.1.27}$$

This also demonstrates that the Dirac equation predicts the Landé factor  $g$  to be exactly double the value of the orbital angular momentum, as shown in eq. (2.0.1). Besides the Lorentz invariance, this prediction is the most remarkable achievement of the Dirac equation.

However, the experimentally determined value for the magnetic moment of the muon deviates from the Dirac-predicted value  $g_\mu = 2$ . It has turned out that there are underlying processes occurring in quantum field theory that have to be confronted to explain this anomaly in  $g_\mu$ . To quantify the deviation from the experiments, the so-called anomalous magnetic moment  $a_\mu$  is introduced as

$$a_\mu = \frac{g_\mu - 2}{2}. \tag{2.1.28}$$

In QED,  $a_\mu$  is dealt with by considering loop-corrections which we will confront in section 2.3. To prepare this, the next section explains what the general structure of the interaction of the muon and an electromagnetic field looks like and how it can be described mathematically.

## 2.2 Extraction of QED form factors

The scattering process from which we will derive any deviations from  $g_\mu$  within the QED is shown in Fig. 2.1.

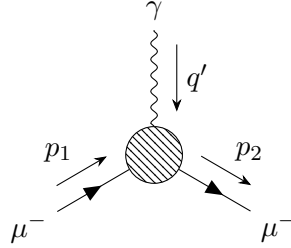


Figure 2.1: Scattering process contributing to  $a_\mu$

The excitement of the electromagnetic field is represented by a photon which scatters an incoming muon. In between those particles, the blob represents all possible corrections that may lead to  $a_\mu$ .

The Lorentz-invariant amplitude  $\mathcal{M} = \epsilon_\sigma \mathcal{M}^\sigma$ , where  $\epsilon_\sigma$  denotes the polarization vector of the incoming photon, is the matrix element that, once squared and summed over spins, gives the physical cross section or decay rate. Thus,  $\mathcal{M}^\sigma$  is an important quantity to determine. It transforms like a Lorentz vector and can therefore be written as a linear combination of all possible Lorentz vectors that can appear in the interaction, namely  $p_1^\sigma, p_2^\sigma$  and the Dirac-matrices  $\gamma^\sigma$  ([6], pp. 202-203). It is our choice to choose two orthogonal linear combinations,  $P^\sigma = p_1^\sigma + p_2^\sigma$  and  $q'^\sigma = p_1^\sigma - p_2^\sigma$ , of the incoming momenta.<sup>2</sup>  $\mathcal{M}^\sigma$  can then be written as<sup>3</sup>

$$\mathcal{M}^\sigma = \bar{u}(p_2) \left\{ \alpha_1 \gamma^\sigma + \frac{\alpha_2}{2m} P^\sigma + \frac{\alpha_3}{2m} q'^\sigma + \alpha_4 \gamma^\sigma \gamma^5 + \frac{\alpha_5}{2m} q'^\sigma \gamma^5 + i \frac{\alpha_6}{2m} P^\sigma \gamma^5 \right\} u(p_1) \quad (2.2.1)$$

For our calculation, only the first three terms are required, as QED is parity invariant. Because of four-momentum conservation,  $q' = p_2 - p_1$  holds. The  $\alpha_i$  can only depend on Lorentz-invariant scalars, i.e. dot products between the incoming and outgoing four-momenta  $p_1, p_2, q'$  and  $\gamma$ .

The following observations help to simplify any expressions that appear in interactions like the one given in Fig. 2.1:

1. The incoming and outgoing muon is on its mass-shell, i.e.

$$p_1^2 = p_2^2 = E^2 - \mathbf{p}_{1/2}^2 = m_\mu^2 \quad (2.2.2)$$

2. Dot products of the  $\gamma$ -matrices with the momenta  $p_i$  and  $q'$ , denoted as  $\not{p}_1, \not{p}_2$  and  $\not{q}'$ , can be rewritten using eq. (2.1.16) and its Dirac adjoint.
3. To perform step 2, it is often required to swap the appearing Lorentz vectors with  $\gamma^5$ . A.1 provides the necessary identities to do so.

With that being said, it becomes evident that the Lorentz-invariant scalars  $\alpha_i$  only depend on particle-related parameters such like masses of any particles involved in the interaction blob. The Ward identity  $q'_\sigma \mathcal{M}^\sigma = 0$  is used in the following to eliminate some of the terms in (2.2.1).

<sup>2</sup>  $P^\sigma q'_\sigma = p_1^2 - p_2^2 \stackrel{(2.2.2)}{=} 0$ .

<sup>3</sup> The appearing  $\gamma^5$ -matrix is introduced in A.1.

$$\begin{aligned}
 0 &\stackrel{!}{=} q'_\sigma \mathcal{M}^\sigma = q'_\sigma \bar{u}(p_2) \left\{ \alpha_1 \gamma^\sigma + \frac{\alpha_2}{2m} P^\sigma + \frac{\alpha_3}{2m} q'^\sigma + \alpha_4 \gamma^\sigma \gamma^5 + \frac{\alpha_5}{2m} q'^\sigma \gamma^5 + i \frac{\alpha_6}{2m} P^\sigma \gamma^5 \right\} u(p_1) \\
 &= \bar{u}(p_2) \left\{ \cancel{\alpha_1 \not{q}} + \frac{\alpha_2}{2m} \cancel{P^\sigma \not{q}'_\sigma} + \frac{\alpha_3}{2m} q'^2 + \alpha_4 \not{q}' \gamma^5 + \frac{\alpha_5}{2m} q'^2 \gamma^5 + i \frac{\alpha_6}{2m} \cancel{P^\sigma \not{q}'_\sigma \gamma^5} \right\} u(p_1) \\
 &= \bar{u}(p_2) \left\{ \frac{\alpha_3}{2m} q'^2 + \left( 2m\alpha_4 + \frac{\alpha_5}{2m} q'^2 \right) \gamma^5 \right\} u(p_1)
 \end{aligned} \tag{2.2.3}$$

In the second step, we used the Dirac equation (2.1.16) and the chosen orthogonality of  $P$  and  $q'$  to eliminate the first, second and last term. The equation is only true if the coefficients fulfill

$$\alpha_3 = 0 \quad \text{and} \quad \alpha_5 = -\frac{4m^2}{q'^2} \alpha_4. \tag{2.2.4}$$

Plugging this into (2.2.1) gives

$$\mathcal{M}^\sigma = \bar{u}(p_2) \left\{ \alpha_1 \gamma^\sigma + \frac{\alpha_2}{2m} P^\sigma + \alpha_4 \left( \gamma^\sigma - \frac{2m}{q'^2} q'^\sigma \right) \gamma^5 + i \frac{\alpha_6}{2m} P^\sigma \gamma^5 \right\} u(p_1) \tag{2.2.5}$$

We can now apply the Gordon decomposition (A.2.1) and its analogue for involved  $\gamma^5$ -matrices (A.2.7) to obtain our final result for the general structure of the amplitude  $\mathcal{M}^\sigma$

$$\begin{aligned}
 \mathcal{M}^\sigma &= \bar{u}(p_2) \left\{ (\alpha_1 + \alpha_2) \gamma^\sigma - i \frac{\alpha_2}{2m} \sigma^{\sigma\nu} p_{-\nu} + \alpha_4 \left( \gamma^\sigma - \frac{2m}{q'^2} q'^\sigma \right) \gamma^5 + i \frac{\alpha_6}{2m} \sigma^{\sigma\nu} q'_\nu \gamma^5 \right\} u(p_1) \\
 &\equiv -ie \bar{u}(p_2) \left\{ \gamma^\sigma F_E(q'^2) + \frac{i}{2m} F_M(q'^2) \sigma^{\sigma\nu} p_{-\nu} + F_A(q'^2) \left( \gamma^\sigma - \frac{2m}{q'^2} q'^\sigma \right) \gamma^5 + \right. \\
 &\quad \left. + \frac{i}{2m} F_D(q'^2) \sigma^{\sigma\nu} p_{-\nu} \right\} u(p_1),
 \end{aligned} \tag{2.2.6}$$

where we introduced the electric charge form factor  $F_E(q'^2)$ , the magnetic form factor  $F_M(q'^2)$ , the anapole moment  $F_A(q'^2)$  and the electric dipole moment  $F_D(q'^2)$  as

$$\begin{aligned}
 F_E(q'^2) &= \frac{i}{e} \left( \alpha_1(q'^2) + \alpha_2(q'^2) \right) \\
 F_M(q'^2) &= -\frac{i}{e} \alpha_2(q'^2) \\
 F_A(q'^2) &= \frac{i}{e} \alpha_4(q'^2) \\
 F_D(q'^2) &= \frac{i}{e} \alpha_6(q'^2)
 \end{aligned} \tag{2.2.7}$$

At tree level the muon-photon vertex “blob” collapses to the bare QED vertex,

$$\mathcal{M}^\sigma = -ie \bar{u}(p_2) \gamma^\sigma u(p_1), \tag{2.2.8}$$

which, when inserted into the low-energy magnetic interaction, produces the familiar Dirac value  $g_\mu = 2$ . In the language of form factors this is equivalent to say that all form factors vanish except the electric (or Dirac) form factor, which is fixed to  $F_E(q'^2 = 0) = 1$ . No magnetic form factor appears at tree level, so  $F_M(q'^2 = 0) = 0$ .

As we will see in the following section, loop corrections in QED modify the vertex by generating a term proportional to the Lorentz tensor  $\sigma^{\sigma\nu} p_\nu$ . When one takes the non-relativistic, static limit  $q'^2 \rightarrow 0$ , this tensor structure reduces to the Pauli interaction  $\frac{e}{2m} \boldsymbol{\sigma} \cdot \mathbf{B}$ , which is exactly the coupling of a magnetic dipole to an external magnetic field. The relativistic amplitude for the interaction,

$$\mathcal{M}^\sigma = -ie \bar{u} \left[ F_E(q'^2) \gamma^\sigma + F_M(q'^2) \frac{i}{2m} \sigma^{\sigma\nu} p_{-\nu} \right] u, \tag{2.2.9}$$

must match the non-relativistic expression for a magnetic moment,  $\boldsymbol{\mu} = g_\mu, (e/2m_\mu), \mathbf{S}$ , in the low-energy limit. This implies that the total strength of the moment is governed by the form factors at zero momentum transfer, yielding the definition:

$$g_\mu \frac{e}{2m_\mu} \equiv [F_E(0) + F_M(0)] \frac{e}{m_\mu} \Rightarrow g_\mu = 2[F_E(0) + F_M(0)]. \quad (2.2.10)$$

Since  $F_E(0) = 1$ , any deviation of  $g_\mu$  from 2 is carried entirely by  $F_M(0)$ . With the definition of the AMM (2.1.28) one immediately can identify

$$a_\mu = F_M(0). \quad (2.2.11)$$

In other words, the Pauli form factor at zero momentum transfer includes all loop-induced corrections to the muon's magnetic moment coupling and its value in the static limit is precisely the anomalous magnetic moment.

## 2.3 One-Loop Contribution within Quantum Electrodynamics

The QED already achieves to predict the value of  $a_\mu$  with an outstanding precision. The corrections of  $g = 2$  are determined via the internal, virtual particle interactions, i.e. photon loops which also appear in the calculation of the magnitude  $\mathcal{M}^\sigma$  and thus in the several form factors, as shown in Section 2.2. We will derive the first order loop correction of  $a_\mu$  by extracting the magnetic form factor evaluated at  $q' = 0$  from the magnitude  $\mathcal{M}^\sigma$ , corresponding to the Feynman diagram 2.2.

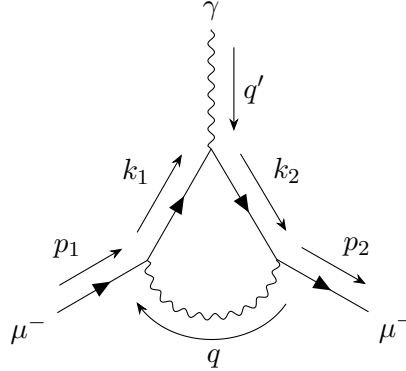


Figure 2.2: One-loop correction diagram in the QED

The scattering amplitude can be derived with the help of the Feynman rules, listed in appendix A.3. For simplicity, the indices  $s$  indicating the spin of the particles and the corresponding momenta  $p_1$  and  $p_2$  will be left out in the following.

$$\begin{aligned} \mathcal{M}^\sigma &= \int \frac{d^4q}{(2\pi)^4} \bar{u}^{s_1}(p_2) \left\{ (i e \gamma_\nu) \left( i \frac{\not{k}_2 + m}{k_2^2 - m^2 + i\varepsilon} \right) (i e \gamma^\sigma) \left( i \frac{\not{k}_1 + m}{k_1^2 - m^2 + i\varepsilon} \right) (i e \gamma_\mu) \times \right. \\ &\quad \left. \times \left( -i \frac{g^{\mu\nu}}{q^2 + i\varepsilon} \right) \right\} u^{s_2}(p_1) \\ &= e^3 \int \frac{d^4q}{(2\pi)^4} \bar{u} \left\{ \gamma_\nu \left( \frac{\not{k}_2 + m}{k_2^2 - m^2 + i\varepsilon} \right) \gamma^\sigma \left( \frac{\not{k}_1 + m}{k_1^2 - m^2 + i\varepsilon} \right) \gamma_\mu \left( \frac{g^{\mu\nu}}{(k_1 - p_1)^2 + i\varepsilon} \right) \right\} u \\ &\stackrel{(A.1.2)}{=} e^3 \int \frac{d^4q}{(2\pi)^4} \bar{u} \left\{ \frac{-2\not{k}_1 \gamma^\sigma \not{k}_2 - 2m^2 \gamma^\sigma + 4m(k_1 + k_2)^\sigma}{(k_1^2 - m^2 + i\varepsilon)(k_2^2 - m^2 + i\varepsilon)((k_1 - p_1)^2 + i\varepsilon)} \right\} u \\ &\equiv e^3 \int \frac{d^4q}{(2\pi)^4} \frac{N^\sigma}{ABC}, \end{aligned} \quad (2.3.1)$$

where we defined the denominator to be a product of

$$\begin{aligned} A &= k_1^2 - m^2 + i\varepsilon, \\ B &= k_2^2 - m^2 + i\varepsilon, \\ C &= (k_1 - p_1)^2 + i\varepsilon. \end{aligned} \quad (2.3.2)$$

This integral can be evaluated using the Feynman method, shown in appendix A.4. We first express the denominator with an integral over the Feynman parameters  $x, y$  and  $z$ :

$$\frac{1}{ABC} = 2 \int_{[0;1]^3} dx dy dz \delta(x + y + z - 1) \frac{1}{D^3(x, y, z)}, \quad (2.3.3)$$

where we compute  $D$  to be of the form

$$\begin{aligned} D &= xA + yB + zC \\ &= ((k_1 - p_1)^2 + i\varepsilon)z + (k_2^2 - m^2 + i\varepsilon)y + (k_1^2 - m^2 + i\varepsilon)x \\ &\stackrel{(2.2.2)}{=} (q^2 + i\varepsilon)z + (\not{p}_2^2 + 2p_2q + q^2 - \not{m}^2 + i\varepsilon)y + (\not{p}_1^2 + 2p_1q + q^2 - \not{m}^2 + i\varepsilon)x \\ &= q^2 \underbrace{(z + y + x)}_{=1} + i\varepsilon \underbrace{(z + y + x)}_{=1} + 2(p_2^\sigma y + p_1^\sigma x)q_\sigma \\ &= (q^\sigma + p_2^\sigma y + p_1^\sigma x)^2 - (p_2 y + p_1 x)^2 + i\varepsilon. \end{aligned} \quad (2.3.4)$$

In step three, we used the fact, that the incoming and outgoing muon is on its mass shell and step four simplifies the sum over the Feynman parameters to one which results from the  $\delta$ -distribution in (2.3.3). We introduce the shifted momentum  $\ell^\sigma$  and  $\Delta$

$$\ell^\sigma = q^\sigma + p_2^\sigma y + p_1^\sigma x \quad (2.3.5)$$

$$\Delta = (p_2^\sigma y + p_1^\sigma x)^2 \quad (2.3.6)$$

to rewrite  $D$  as

$$D \equiv \ell^2 - \Delta + i\varepsilon. \quad (2.3.7)$$

Using energy and momentum conservation we obtain that  $(p_2 - p_1) \rightarrow 0$  which shows that  $p_1 p_2 = m^2$  and that (2.3.6) can be rewritten in terms of

$$\Delta = m^2(x + y)^2. \quad (2.3.8)$$

We can now deal with the numerator as follows:

$$N^\sigma = \bar{u} \left\{ \underbrace{-2(\not{p}_1 + \not{q}) \gamma^\sigma (\not{p}_2 + \not{q})}_{(1)} - \underbrace{2m^2 \gamma^\sigma}_{(2)} + \underbrace{4m(p_1^\sigma + p_2^\sigma + 2q^\sigma)}_{(3)} \right\} u \quad (2.3.9)$$

The first term can be simplified by expanding the  $\gamma$ -matrices by the help of the relation (A.1.2):

$$\begin{aligned} (1) &= \bar{u} \left\{ -2(p_1 + q)_\mu \gamma^\mu \gamma^\sigma \gamma^\nu (p_2 + q)_\nu \right\} u \\ &= \bar{u} \left\{ -2(p_1 + q)_\mu [2(g^{\sigma\nu} \gamma^\mu - g^{\mu\nu} \gamma^\sigma + g^{\mu\sigma} \gamma^\nu) - \gamma^\nu \gamma^\sigma \gamma^\mu] (p_2 + q)_\nu \right\} u \\ &= \bar{u} \left\{ -4(\not{p}_1 + \not{q})(p_2^\sigma + q^\sigma) + 4(p_1 + q)^\nu (p_2 + q)_\nu \gamma^\sigma - 4(p_1^\sigma + q^\sigma)(\not{p}_2 + \not{q}) + \right. \\ &\quad \left. + 2(\not{p}_2 + \not{q}) \gamma^\sigma (\not{p}_1 + \not{q}) \right\} u \end{aligned} \quad (2.3.10)$$

Applying the Dirac equation (2.1.16) and its Dirac adjoint yields

$$(1) = \bar{u} \left\{ \underbrace{-4m(p_1^\sigma + p_2^\sigma + 2q^\sigma)}_{(i)} + 4(p_1 p_2 + p_1 q + p_2 q + q^2) \gamma^\sigma - 4\not{q}(p_1^\sigma + p_2^\sigma + 2q^\sigma) + \right. \\ \left. + 2 \left( \underbrace{m^2 \gamma^\sigma}_{(ii)} + m \underbrace{(\gamma^\sigma \not{q} + \not{q} \gamma^\sigma)}_{\stackrel{(A.1.1)}{=} 2g^{\sigma\nu} q_\nu = 2q^\sigma} + \not{q} \gamma^\sigma \not{q} \right) \right\} u. \quad (2.3.11)$$

Expanding and using (A.1.2) once more gives

$$\not{q} \gamma^\sigma \not{q} = 2q^\sigma \not{q} - q^2 \gamma^\sigma \quad (2.3.12)$$

and thus

$$(1) = \bar{u} \left\{ (i) + 2(ii) + 4(p_1 p_2 + p_1 q + p_2 q) \gamma^\sigma + 2q^2 \gamma^\sigma - 4\not{q}(p_1^\sigma + p_2^\sigma) - 4\not{q} q^\sigma \right\} u. \quad (2.3.13)$$

Inserting (2.3.13) into (2.3.9) gives the simplified numerator

$$N^\sigma = \bar{u} \left\{ 2\gamma^\sigma (q^2 + 2(p_1 p_2 + p_1 q + p_2 q)) - 4\not{q}(p_1^\sigma + p_2^\sigma + q^\sigma) + 4mq^\sigma \right\} u, \quad (2.3.14)$$

as (i) and 2(ii) cancel out with the second and third term in (2.3.9).

The next step is to insert the momentum shift (2.3.5), i.e.

$$q = \ell - (p_2 y + p_1 x) \quad (2.3.15)$$

into the numerator, which gives

$$N^\sigma = \bar{u} \left\{ 2\gamma^\sigma \left[ \ell^2 - 2\ell^\mu (p_{2\mu} y + p_{1\mu} x) + (p_2^\mu y + p_1^\mu x)^2 + 2(p_1 p_2 + (p_1 + p_2)_\mu (\ell^\mu - p_2^\mu y - p_1^\mu x)) \right] - \right. \\ \left. - 4(\ell - p_2 y - p_1 x)(p_1^\sigma + p_2^\sigma + \ell^\sigma - p_2^\sigma y - p_1^\sigma x) + 4m(\ell^\sigma - p_2^\sigma y - p_1^\sigma x) \right\} u.$$

The denominator in the integration (2.3.1) only depends on  $\ell^2$ . Because of symmetry, every term in the numerator being linear in  $\ell$  does not contribute to the integral. Furthermore, it can be shown that ([7], p. 191)

$$\int \frac{d^4 \ell}{(2\pi)^4} \ell^\mu \ell^\nu = \int \frac{d^4 \ell}{(2\pi)^4} \frac{1}{4} g^{\mu\nu} \ell^2. \quad (2.3.16)$$

Thus, we can only regard the contributing part of  $N^\sigma$  and simplify it as follows:

$$N_{\text{cont}}^\sigma = \bar{u} \left\{ 2\gamma^\sigma \left[ \ell^2 + (p_2^\mu y + p_1^\mu x)^2 + 2(p_1 p_2 - (p_{1\mu} + p_{2\mu})(p_2^\mu y + p_1^\mu x)) \right] + \right. \\ \left. + 4(p_2 y + p_1 x)(p_1^\sigma + p_2^\sigma - p_2^\sigma y - p_1^\sigma x) - \underbrace{4\frac{1}{4} g_\mu^\sigma \gamma^\mu \ell^2}_{\ell^2 \gamma^\sigma} - 4m(p_2^\sigma y + p_1^\sigma x) \right\} u \\ \stackrel{(2.1.16)}{=} \bar{u} \left\{ \left[ \ell^2 + 2p_2^2 y(y-2) + 2p_1^2 x(x-2) + 4p_1 p_2(xy + 2(1-y-x)) \right] \gamma^\sigma + \right. \\ \left. + 4m \left[ (y+x)(p_1(1-x) + p_2(1-y))^\sigma - (p_2^\sigma y + p_1^\sigma x) \right] \right\} u \\ = \bar{u} \left\{ \underbrace{\left[ \ell^2 + 2m^2(y(y-2) + x(x-2)) + 4p_1 p_2(xy + 2z) \right]}_{\tilde{\gamma}^\sigma} \gamma^\sigma + \right. \\ \left. + 4m \left[ (x+y)(p_1^\sigma + p_2^\sigma) - (p_1^\sigma x + p_2^\sigma y)(1+x+y) \right] \right\} u. \quad (2.3.17)$$

We can now express the momenta  $p_1$  and  $p_2$  in the following way

$$\begin{aligned} p_1^\sigma &= \frac{1}{2} [(p_1^\sigma + p_2^\sigma) + (p_1^\sigma - p_2^\sigma)] \equiv \frac{1}{2} (p_+^\sigma + p_-^\sigma) \\ p_2^\sigma &= \frac{1}{2} [(p_1^\sigma + p_2^\sigma) - (p_1^\sigma - p_2^\sigma)] \equiv \frac{1}{2} (p_+^\sigma - p_-^\sigma), \end{aligned} \quad (2.3.18)$$

which we can use to rearrange  $N_{\text{cont}}^\sigma$ :

$$\begin{aligned} N_{\text{cont}}^\sigma &= \bar{u} \left[ \bar{\gamma}^\sigma + 4m(x+y)p_+^\sigma - 4m(1+x+y) \left[ \frac{x}{2}(p_+^\sigma + p_-^\sigma) + \frac{y}{2}(p_+^\sigma - p_-^\sigma) \right] \right] u \\ &= \bar{u} \left[ \bar{\gamma}^\sigma + 4m(x+y) \left[ 1 - \frac{1}{2}(1+x+y) \right] p_+^\sigma - 2m(1+x+y)(x-y)p_-^\sigma \right] u \\ &= \bar{u} \left[ \bar{\gamma}^\sigma + 2m(x+y)(1-x-y)p_+^\sigma - 2m(1+x+y)(x-y)p_-^\sigma \right] u. \end{aligned} \quad (2.3.19)$$

Finally, we can apply the Gordon decomposition (A.2.1) and substitute

$$p_+^\sigma = 2m\gamma^\sigma - i\sigma^{\sigma\nu}p_{-\nu}. \quad (2.3.20)$$

As discussed in Section 2.2, only the term proportional to  $\sigma^{\sigma\nu}p_{-\nu}$  contributes to the AMM. Thus, every other term can be neglected and we are left with the AMM-contributing part of the numerator  $N^\sigma$

$$N_{\text{AMM}}^\sigma = \bar{u} \left\{ -2m(x+y)(x+y-1)i\sigma^{\sigma\nu}p_{-\nu} \right\} u. \quad (2.3.21)$$

By inserting (2.3.21) into (2.3.1) and comparing the result with the general form of the scattering amplitude (2.2.6), we obtain

$$e^3 \int \frac{N_{\text{AMM}}^\sigma}{ABC} \frac{d^4\ell}{(2\pi)^4} \stackrel{!}{=} -ie\bar{u} \left\{ i\frac{1}{2m}\sigma^{\sigma\nu}p_{-\nu}F_M(q') \right\} u. \quad (2.3.22)$$

By the help of the Feynman trick for the denominator (2.3.3), the form factor  $F_M(q')$  can be read of as

$$F_M(q') = i4me^2 \int \frac{d^4\ell}{(2\pi)^4} \int_{[0;1]^3} dx dy dz \delta(x+y+z-1) \frac{-2m(x+y)(x+y-1)}{D^3}, \quad (2.3.23)$$

with  $D$  being given in (2.3.7). We can solve the integral over the momenta using the following general formula ([7], p. 193):

$$\int \frac{d^4\ell}{(2\pi)^4} \frac{1}{(\ell^2 - \Delta)^n} = (-1)^n \frac{i}{(4\pi)^2} \frac{1}{(n-1)(n-2)} \frac{1}{\Delta^{n-2}}. \quad (2.3.24)$$

Our study makes use of the case  $n = 3$ , for which we obtain

$$\int_0^\infty \frac{d^4\ell}{(2\pi)^4} \frac{1}{(\ell^2 - \Delta + i\varepsilon)^3} \stackrel{\varepsilon \rightarrow 0}{=} -\frac{i}{32\pi^2} \frac{1}{\Delta} \quad (2.3.25)$$

Plugging this into (2.3.23) gives

$$\begin{aligned} F_M(q') &= 8im^2e^2 \int \frac{d^4\ell}{(2\pi)^4} \int_{[0;1]^3} dx dy dz \delta(x+y+z-1) \frac{(1-z)z}{D^3} \\ &= \frac{8e^2m^2}{32\pi^2} \iiint_0^1 dx dy dz \delta(x+y+z-1) \frac{z(z-1)}{\Delta} \\ &\stackrel{(2.3.8)}{=} \frac{e^2}{4\pi^2} \iiint_0^1 dx dy dz \delta(x+y+z-1) \frac{z}{1-z}, \end{aligned} \quad (2.3.26)$$

where we considered  $q'$  to be zero in the last step. To evaluate the  $\delta$ -function over  $x$  to one,  $x = 1 - y - z$  must be within  $[0; 1]$ . Therefore, we obtain

$$\begin{aligned} 0 &\leq y + z \leq 1 \\ -z &\leq y \leq 1 - z, \end{aligned}$$

and since the initial integration range  $0 \leq y \leq 1$  must still be satisfied, the integration over  $y$  is now restricted to  $[0; 1 - z]$ . Hence, we obtain

$$F_M(0) = \frac{\alpha}{\pi} \int_0^{1-z} dy \int_0^1 \frac{z}{1-z} dz = \frac{\alpha}{\pi} \int_0^1 z dz = \frac{\alpha}{2\pi}, \quad (2.3.27)$$

after substituting the fine structure constant  $\alpha = e^2/(4\pi)$ .

### 3 One-Loop Contributions from Scalar-Fermion Interactions

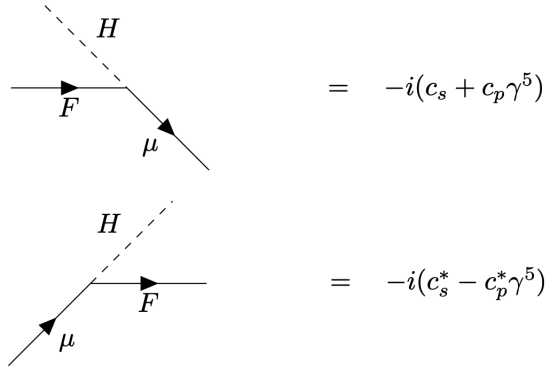
The persistent discrepancy between the measured value of the muon’s AMM,  $a_\mu = (g_\mu - 2)/2$ , and its SM prediction has become one of the clearest hints of physics BSM. In this chapter we shall focus on a minimal class of BSM scenarios in which new scalar fields couple to muons and additional fermions. Our goal is to show how these extra interactions enter the muon’s electromagnetic vertex at one-loop order and to extract the magnetic form factor  $F_M(q^2)$ , whose value at  $q^2 = 0$  directly contributes to  $a_\mu$ , from the internal scalar and fermion lines.

Any new particle which couples to both the muon and the photon can generate an extra contribution to the muon’s magnetic moment via loop interactions of the type shown in Section 2.3. In particular, if we introduce a new neutral or charged scalar  $H$  together with a fermion  $F$ , then the Yukawa-Lagrangian is given by [8]:

$$\mathcal{L}_{\text{Yuk}} = \sum_{F,H} \overline{\mu}^- (c_s + c_p \gamma^5) F H + H^* \overline{F} (c_s^* - c_p^* \gamma^5) \mu^-, \quad (3.0.1)$$

where  $\mu, F$  and  $H$  denote the corresponding vector- or scalar-like gauge fields and  $c_s$  and  $c_p$  are the scalar and pseudoscalar coupling constants, respectively.

The Lagrangian can be used to extract the needed Feynman rules for the newly appearing vertices for the charged scalar bosons:



With those rules set up, we are ready to turn to explicit one-loop integrals, evaluate them using standard Feynman parameter techniques and derive analytical expressions for the new-physics contribution to  $a_\mu$ .

### 3.1 Interaction of a charged fermion with the EM field

The first topology considers the interaction of an internal charged fermion  $F$  with a photon of the electromagnetic field, as shown in Fig. 3.1:

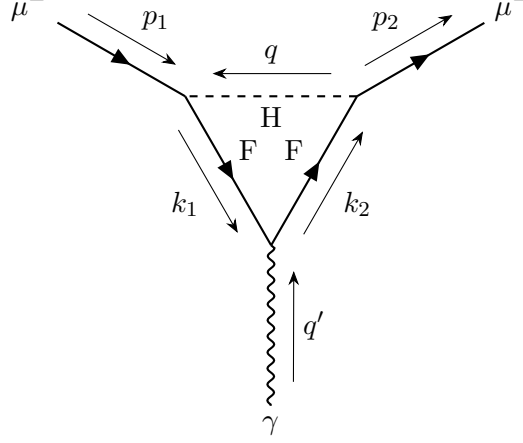


Figure 3.1: Absorption of a photon via the internal Fermion Line

In the following, the contribution to the AMM  $a_\mu$  from interaction 3.1 is derived from the corresponding invariant amplitude  $\mathcal{M} = \epsilon_\sigma \mathcal{M}^\sigma$ . Using the Feynman rules, we derive

$$\begin{aligned}
 \mathcal{M}^\sigma &= \int \frac{d^4q}{(2\pi)^4} \bar{u}(p_2) i(c_s + c_p \gamma^5) \frac{i(\not{k}_2 + m_F)}{k_2^2 - m_F^2 + i\varepsilon} i q_F \gamma^\sigma \frac{i(\not{k}_1 + m_F)}{k_1^2 - m_F^2 + i\varepsilon} i(c_s^* - c_p^* \gamma^5) \times \\
 &\quad \times \frac{i}{q^2 - m_H^2 + i\varepsilon} u(p_1) \\
 &= -q_F \int \frac{d^4q}{(2\pi)^4} \bar{u} \frac{(c_s + c_p \gamma^5) (\not{k}_2 + m_F) \gamma^\sigma (\not{k}_1 + m_F) (c_s^* - c_p^* \gamma^5)}{(k_2^2 - m_F^2 + i\varepsilon) (k_1^2 - m_F^2 + i\varepsilon) (q^2 - m_H^2 + i\varepsilon)} u \\
 &\equiv -q_F \int \frac{N^\sigma}{ABC} \frac{d^4q}{(2\pi)^4}. \tag{3.1.1}
 \end{aligned}$$

The denominator can again be rewritten using the Feynman trick as follows:

$$\begin{aligned}
 \frac{1}{ABC} &= 2 \iiint_0^1 dx dy dz \delta(x + y + z - 1) \frac{1}{(Ax + By + Cz)^3} \\
 &\equiv 2 \iiint_0^1 dx dy dz \delta(x + y + z - 1) \frac{1}{D^3} \\
 \text{where } D &= (q^2 - m_H^2 + i\varepsilon)x + (k_2^2 - m_F^2 + i\varepsilon)y + (k_1^2 - m_F^2 + i\varepsilon)z. \tag{3.1.2}
 \end{aligned}$$

Inserting four momentum conservation  $k_i = q + p_i$  and (A.4.2) yields

$$\begin{aligned}
 D &= q^2 + i\varepsilon - m_H^2 x + p_2^2 y + p_1^2 z - m_F^2 (1 - x) + 2q_\mu (p_2 y + p_1 z)^\mu \\
 &\stackrel{(2.2.2)}{=} (q^\mu + p_2^\mu y + p_1^\mu z)^2 - (p_2^\mu y + p_1^\mu z)^2 - m_H^2 x + m_\mu^2 (1 - x) - m_F^2 (1 - x) + i\varepsilon \\
 D &\equiv \ell^2 - \Delta + i\varepsilon, \tag{3.1.3}
 \end{aligned}$$

with the shifted momentum  $\ell$  and  $\Delta$  to be defined as

$$\ell = q + p_2 y + p_1 z \tag{3.1.4}$$

$$\Delta = m_\mu^2 (y^2 + z^2) + 2p_1 p_2 y z + m_H^2 x - (1 - x)(m_\mu^2 - m_F^2) + i\varepsilon. \tag{3.1.5}$$

We again use four-momentum conservation to express  $k_i = q + p_i$  and insert the shifted momentum  $q$  via (3.1.4):

$$\begin{aligned} N^\sigma &= \bar{u} \left\{ (c_s + c_p \gamma^5) (\not{k}_2 + m_F) \gamma^\sigma (\not{k}_1 + m_F) (c_s^* - c_p^* \gamma^5) \right\} u \\ &= \bar{u} \left\{ (c_s + c_p \gamma^5) (\not{p}_2 + \not{\ell} - \not{p}_2 y - \not{p}_1 z + m_F) \gamma^\sigma (\not{p}_1 + \not{\ell} - \not{p}_2 y - \not{p}_1 z + m_F) (c_s^* - c_p^* \gamma^5) \right\} u. \end{aligned}$$

The terms linear in  $\ell$  can again be left out, as they will disappear in the integral due to symmetry. This leaves us with

$$\begin{aligned} N_{\text{cont}}^\sigma &= \bar{u} \left\{ (c_s + c_p \gamma^5) \left[ \not{\ell} \gamma^\sigma \not{\ell} + (\not{p}_2(1-y) - \not{p}_1 z + m_F) \gamma^\sigma (\not{p}_1(1-z) - \not{p}_2 y + m_F) \right] \times \right. \\ &\quad \left. \times (c_s^* - c_p^* \gamma^5) \right\} u \\ &= \bar{u} \left\{ (c_s + c_p \gamma^5) \left[ \underbrace{\not{\ell} \gamma^\sigma \not{\ell} + (\not{p}_2(1-y) - \not{p}_1 z) \gamma^\sigma (\not{p}_1(1-z) - \not{p}_2 y) + m_F^2 \gamma^\sigma}_{\Gamma_{\text{odd}}^\sigma} + \right. \right. \\ &\quad \left. \left. + \underbrace{m_F \gamma^\sigma (\not{p}_1(1-z) - \not{p}_2 y) + m_F (\not{p}_2(1-y) - \not{p}_1 z) \gamma^\sigma}_{\Gamma_{\text{even}}^\sigma} (c_s^* - c_p^* \gamma^5) \right] \right\} u. \end{aligned} \quad (3.1.6)$$

$\Gamma_{\text{odd}}^\sigma$  and  $\Gamma_{\text{even}}^\sigma$  denote those terms, that include a respective odd and even number of  $\gamma$ -matrices. We will continue treating them separately.

$$\bar{u} (c_s + c_p \gamma^5) \Gamma_{\text{odd}}^\sigma (c_s^* - c_p^* \gamma^5) u = \bar{u} \left[ |c_s|^2 \Gamma_{\text{odd}}^\sigma - |c_p|^2 \gamma^5 \Gamma_{\text{odd}}^\sigma \gamma^5 - c_s c_p^* \Gamma_{\text{odd}}^\sigma \gamma^5 + c_p c_s^* \gamma^5 \Gamma_{\text{odd}}^\sigma \right] u \quad (3.1.7)$$

$$\bar{u} (c_s + c_p \gamma^5) \Gamma_{\text{even}}^\sigma (c_s^* - c_p^* \gamma^5) u = \bar{u} \left[ |c_s|^2 \Gamma_{\text{even}}^\sigma - |c_p|^2 \gamma^5 \Gamma_{\text{even}}^\sigma \gamma^5 - c_s c_p^* \Gamma_{\text{even}}^\sigma \gamma^5 + c_p c_s^* \gamma^5 \Gamma_{\text{even}}^\sigma \right] u \quad (3.1.8)$$

Recalling the (anti-)commutation relation of the  $\gamma^5$ -matrix (A.1.4) and inserting  $\Gamma_{\text{odd}}^\sigma$  into eq. (3.1.7) enables us to factor  $\Gamma_{\text{odd}}^\sigma$  out. With the Dirac equation (2.1.16) and the properties of the  $\gamma$ -matrix we can simplify the resulting expression as follows:

$$\begin{aligned} &\bar{u} \left\{ (|c_s|^2 + |c_p|^2) \left[ -\frac{1}{2} \ell^2 \gamma^\sigma + (m_\mu(1-y) - \not{p}_1 z) \gamma^\sigma (m_\mu(1-z) - \not{p}_2 y) + m_F^2 \gamma^\sigma \right] + \right. \\ &\quad \left. + \underbrace{\gamma^5 \Gamma_{\text{odd}}^\sigma (c_s c_p^* + c_s^* c_p)}_{\equiv \Delta_{\text{odd}}^\sigma} \right\} u \\ &= \bar{u} \left\{ (|c_s|^2 + |c_p|^2) \left[ \left( -\frac{1}{2} \ell^2 + m_F^2 + m_\mu^2(1-y)(1-z) \right) \gamma^\sigma - m_\mu(1-y)y(2p_2^\sigma - m_\mu \gamma^\sigma) - \right. \right. \\ &\quad \left. \left. - m_\mu(1-z)z(2p_1^\sigma - m_\mu \gamma^\sigma) + yz(2m_\mu(p_1^\sigma + p_2^\sigma) - 2p_1 p_2 \gamma^\sigma - m_\mu^2 \gamma^\sigma) \right] + \Delta_{\text{odd}}^\sigma \right\} u \\ &= \bar{u} \left\{ (|c_s|^2 + |c_p|^2) \left[ \left( -\frac{1}{2} \ell^2 + m_F^2 + m_\mu^2(1-y^2 - z^2) - 2p_1 p_2 yz \right) \gamma^\sigma - \right. \right. \\ &\quad \left. \left. - 2m_\mu(xz p_1^\sigma + xy p_2^\sigma) \right] + \Delta_{\text{odd}}^\sigma \right\} u \end{aligned} \quad (3.1.9)$$

The term containing the mixed coupling constants and named  $\Delta_{\text{odd}}^\sigma$  is dealt with later as it requires further identities involving the  $\gamma^5$ -matrix. First, let us consider eq. (3.1.8) and handle it analogously:

$$\begin{aligned} &\bar{u} \left\{ (|c_s|^2 - |c_p|^2) \left[ m_F \gamma^\sigma (\not{p}_1(1-z) - \not{p}_2 y) + m_F (\not{p}_2(1-y) - \not{p}_1 z) \gamma^\sigma \right] \right. \\ &\quad \left. - \underbrace{\gamma^5 \Gamma_{\text{even}}^\sigma (c_s c_p^* - c_s^* c_p)}_{\equiv \Delta_{\text{even}}^\sigma} \right\} u \end{aligned}$$

$$\begin{aligned}
 &= \bar{u} \left\{ (|c_s|^2 - |c_p|^2) m_F \left[ m_\mu (1+x) \gamma^\sigma - y(2p_2^\sigma - m_\mu \gamma^\sigma) - z(2p_1^\sigma - m_\mu \gamma^\sigma) \right] - \Delta_{\text{even}}^\sigma \right\} \\
 &= \bar{u} \left\{ (|c_s|^2 - |c_p|^2) m_F \left[ 2m_\mu \gamma^\sigma - 2(y p_2^\sigma + z p_1^\sigma) \right] - \Delta_{\text{even}}^\sigma \right\}
 \end{aligned} \tag{3.1.10}$$

Again, the term involving products of both coupling constants was labeled as  $\Delta_{\text{even}}^\sigma$ . Both  $\Delta_{\text{odd}}^\sigma$  and  $\Delta_{\text{even}}^\sigma$  are proportional to  $\gamma^5$  and will thus not contribute to the AMM in further calculations. We continue simplifying both terms just for completeness.

$\Delta_{\text{odd}}^\sigma$  between the spinors can be expanded as follows:

$$\begin{aligned}
 \bar{u} \Delta_{\text{odd}}^\sigma u &= \bar{u} \left\{ 2 \operatorname{Re}(c_s c_p^*) \gamma^5 \Gamma_{\text{odd}}^\sigma \right\} u \\
 &= \bar{u} \left\{ 2 \operatorname{Re}(c_s c_p^*) \gamma^5 \left[ \not{\ell} \gamma^\sigma \not{\ell} + (\not{p}_2 (1-y) - \not{p}_1 z) \gamma^\sigma (\not{p}_1 (1-z) - \not{p}_2 y) + m_F^2 \gamma^\sigma \right] \right\} u \\
 &= \bar{u} \left\{ 2 \operatorname{Re}(c_s c_p^*) \gamma^5 \left[ (\not{\ell} \gamma^\sigma \not{\ell} + (x+y z) \not{p}_2 \gamma^\sigma \not{p}_1 - (1-y) y \not{p}_2 \gamma^\sigma \not{p}_2 - \right. \right. \\
 &\quad \left. \left. - z(1-z) \not{p}_1 \gamma^\sigma \not{p}_1 + y z \not{p}_1 \gamma^\sigma \not{p}_2) + m_F^2 \gamma^\sigma \right] \right\} u
 \end{aligned} \tag{3.1.11}$$

The separate terms involving  $\gamma$ -matrices can be rewritten as follows:

$$\bar{u} (\gamma^5 \not{\ell} \gamma^\sigma \not{\ell}) u \stackrel{(A.1.2)}{=} \bar{u} [\gamma^5 (2\not{\ell} \not{\ell}^\sigma - \not{\ell}^2 \gamma^\sigma)] u \stackrel{(2.3.16)}{\stackrel{(A.1.4)}{=}} \bar{u} \left( \frac{1}{2} \not{\ell}^2 \gamma^\sigma \gamma^5 \right) u, \tag{3.1.12}$$

$$\bar{u} (\gamma^5 \not{p}_2 \gamma^\sigma \not{p}_1) u \stackrel{(2.1.16)}{\stackrel{(A.1.4)}{=}} \bar{u} (m_\mu^2 \gamma^\sigma \gamma^5) u, \tag{3.1.13}$$

$$\bar{u} (\gamma^5 \not{p}_2 \gamma^\sigma \not{p}_2) u \stackrel{(A.1.4)}{\stackrel{(2.1.16)}{=}} \bar{u} (-m_\mu \gamma^5 \gamma^\sigma \not{p}_2) u \stackrel{(A.1.1)}{\stackrel{(2.1.16)}{=}} \bar{u} (-2m_\mu p_2^\sigma \gamma^5 + m_\mu^2 \gamma^\sigma \gamma^5) u, \tag{3.1.14}$$

$$\bar{u} (\gamma^5 \not{p}_1 \gamma^\sigma \not{p}_1) u \stackrel{(2.1.16)}{\stackrel{(A.1.1)}{=}} \bar{u} (m_\mu \gamma^5 (2p_1^\sigma - \gamma^\sigma \not{p}_1)) u \stackrel{(A.1.4)}{\stackrel{(2.1.16)}{=}} \bar{u} (m_\mu^2 \gamma^\sigma \gamma^5 + 2m_\mu p_1^\sigma \gamma^5) u, \tag{3.1.15}$$

$$\begin{aligned}
 \bar{u} (\gamma^5 \not{p}_1 \gamma^\sigma \not{p}_2) u &\stackrel{(A.1.2)}{=} \bar{u} \left[ \gamma^5 \left( 2(p_1^\sigma \not{p}_2 + p_2^\sigma \not{p}_1 - p_1 p_2 \gamma^\sigma) - \not{p}_2 \gamma^\sigma \not{p}_1 \right) \right] u \\
 &\stackrel{(A.1.4)}{\stackrel{(2.1.16)}{=}} \bar{u} \left[ \left( (2p_1 p_2 - m_\mu^2) \gamma^\sigma + 2m_\mu (p_2 - p_1)^\sigma \right) \gamma^5 \right] u.
 \end{aligned} \tag{3.1.16}$$

By the help of the relations above, (3.1.11) can be rearranged as follows:

$$\begin{aligned}
 &\bar{u} \left\{ 2 \operatorname{Re}(c_s c_p^*) \left[ \left( \frac{1}{2} \not{\ell}^2 + (x+y z) m_\mu^2 - (1-y) y m_\mu^2 - (1-z) z m_\mu^2 + y z (2p_1 p_2 - m_\mu^2) - \right. \right. \right. \\
 &\quad \left. \left. - m_F \right) \gamma^\sigma + 2m_\mu (1-y) y p_2^\sigma - 2m_\mu (1-z) z p_1^\sigma + 2m_\mu y z (p_2 - p_1)^\sigma \right] \gamma^5 \right\} u \\
 &= \bar{u} \left\{ 2 \operatorname{Re}(c_s c_p^*) \left[ \left( \frac{1}{2} \not{\ell}^2 + m_\mu^2 (2x + y^2 + z^2 - 1) + 2p_1 p_2 y z - m_F^2 \right) \gamma^\sigma + \right. \right. \\
 &\quad \left. \left. + 2m_\mu (p_2^\sigma y (x+2z) - p_1^\sigma z (x+2y)) \right] \gamma^5 \right\} u.
 \end{aligned} \tag{3.1.17}$$

$\Delta_{\text{even}}^\sigma$  between the spinors yields

$$\begin{aligned}
 \bar{u} \Delta_{\text{even}}^\sigma u &= \bar{u} \left\{ \gamma^5 \Gamma_{\text{even}}^\sigma \operatorname{Im}(c_s c_p^*) \right\} u \\
 &= \bar{u} \left\{ 2i \operatorname{Im}(c_s c_p^*) \gamma^5 \left[ m_F \gamma^\sigma (\not{p}_1 (1-z) - \not{p}_2 y) + m_F (\not{p}_2 (1-y) - \not{p}_1 z) \gamma^\sigma \right] \right\} u \\
 &= \bar{u} \left\{ 2i \operatorname{Im}(c_s c_p^*) m_F \left[ (1-z) \gamma^5 \gamma^\sigma \not{p}_1 - y \gamma^5 \gamma^\sigma \not{p}_2 + (1-y) \gamma^5 \not{p}_2 \gamma^\sigma - z \gamma^5 \not{p}_1 \gamma^\sigma \right] \right\} u
 \end{aligned} \tag{3.1.18}$$

Analogously to the even appearances of  $\gamma$ -matrices above, we derive

$$\begin{aligned}
 \bar{u} (\gamma^5 \gamma^\sigma \not{p}_1) u &= -m_\mu \bar{u} (\gamma^\sigma \gamma^5) u, \\
 \bar{u} (\gamma^5 \gamma^\sigma \not{p}_2) u &= \bar{u} [\gamma^5 (2p_2^\sigma - \not{p}_2 \gamma^\sigma)] u = \bar{u} [(2p_2^\sigma - m_\mu \gamma^\sigma) \gamma^5] u, \\
 \bar{u} (\gamma^5 \not{p}_2 \gamma^\sigma) u &= m_\mu \bar{u} (\gamma^\sigma \gamma^5) u, \\
 \bar{u} (\gamma^5 \not{p}_1 \gamma^\sigma) u &= \bar{u} [\gamma^5 (2p_1^\sigma - \gamma^\sigma \not{p}_1)] u = \bar{u} [(2p_1^\sigma + m_\mu \gamma^\sigma) \gamma^5] u
 \end{aligned} \tag{3.1.19}$$

for the odd number of appearances to simplify (3.1.18):

$$\begin{aligned}
 & \bar{u} \left\{ 2i \operatorname{Im}(c_s c_p^*) m_F \left[ -m_\mu (1-z) \gamma^\sigma - y (2p_2^\sigma - m_\mu \gamma^\sigma) + (1-y) m_\mu \gamma^\sigma - \right. \right. \\
 & \quad \left. \left. - z (2p_1^\sigma + m_\mu \gamma^\sigma) \right] \gamma^5 \right\} u \\
 & = \bar{u} \left\{ 4i \operatorname{Im}(c_s c_p^*) m_F (p_2^\sigma y + p_1^\sigma z) \gamma^5 \right\} u.
 \end{aligned} \tag{3.1.20}$$

The results (3.1.9), (3.1.10), (3.1.17) and (3.1.20) can now be combined to form the (contributing) numerator  $N_{\text{cont}}^\sigma$ :

$$\begin{aligned}
 N_{\text{cont}}^\sigma & = \bar{u} \left\{ \left[ \left( -\frac{1}{2} \ell^2 + m_F^2 + m_\mu^2 (1-y^2-z^2) - 2p_1 p_2 y z \right) \gamma^\sigma - 2m_\mu (x z p_1^\sigma + x y p_2^\sigma) \right] \times \right. \\
 & \quad \times (|c_s|^2 + |c_p|^2) + \left[ 2m_F m_\mu \gamma^\sigma - 2m_F (y p_2^\sigma + z p_1^\sigma) \right] (|c_s|^2 - |c_p|^2) + \\
 & \quad + \left[ \operatorname{Re}(c_s c_p^*) \left[ (\ell^2 + 2m_\mu^2 (2x + y^2 + z^2 - 1) + 4p_1 p_2 y z - 2m_F^2) \gamma^\sigma + \right. \right. \\
 & \quad \left. \left. + 4m_\mu (p_2^\sigma y (x + 2z) - p_1^\sigma z (x + 2y)) \right] + 4i \operatorname{Im}(c_s c_p^*) m_F (p_2^\sigma y + p_1^\sigma z) \right] \gamma^5 \left. \right\} u \\
 & = \bar{u} \left\{ \left[ \left( -\frac{1}{2} \ell^2 + m_F^2 + m_\mu^2 (1-y^2-z^2) - 2p_1 p_2 y z \right) (|c_s|^2 + |c_p|^2) + \right. \right. \\
 & \quad + 2m_F m_\mu (|c_s|^2 - |c_p|^2) \left. \right] \gamma^\sigma - \\
 & \quad - 2 \left[ (|c_s|^2 + |c_p|^2) m_\mu x + (|c_s|^2 - |c_p|^2) m_F \right] p_1^\sigma z - \\
 & \quad - 2 \left[ (|c_s|^2 + |c_p|^2) m_\mu x + (|c_s|^2 - |c_p|^2) m_F \right] p_2^\sigma y + \\
 & \quad + \left[ 2 \left( 2i \operatorname{Im}(c_s c_p^*) m_F - 2m_\mu \operatorname{Re}(c_s c_p^*) (x + 2y) \right) p_1^\sigma z + \right. \\
 & \quad + 2 \left( 2i \operatorname{Im}(c_s c_p^*) m_F + 2m_\mu \operatorname{Re}(c_s c_p^*) (x + 2z) \right) p_2^\sigma y + \\
 & \quad \left. + \operatorname{Re}(c_s c_p^*) \left( \ell^2 + 2m_\mu (2x + y^2 + z^2 - 1) + 4p_1 p_2 y z - 2m_F^2 \right) \gamma^\sigma \right] \gamma^5 \left. \right\} u \\
 & \equiv \bar{u} \left\{ A \gamma^\sigma - 2B (p_1^\sigma z + p_2^\sigma y) + \left( \alpha \gamma^\sigma + 2\beta^{(p_1)} p_1^\sigma z + 2\beta^{(p_2)} p_2^\sigma y \right) \gamma^5 \right\} u
 \end{aligned} \tag{3.1.21}$$

where the following abbreviations were introduced:

$$\begin{aligned}
 A & \equiv \left( -\frac{1}{2} \ell^2 + m_F^2 + m_\mu^2 (1-y^2-z^2) - 2p_1 p_2 y z \right) (|c_s|^2 + |c_p|^2) + 2m_F m_\mu (|c_s|^2 - |c_p|^2) \\
 B & \equiv (|c_s|^2 + |c_p|^2) m_\mu x + (|c_s|^2 - |c_p|^2) m_F \\
 \alpha & \equiv \operatorname{Re}(c_s c_p^*) \left( \ell^2 + 2m_\mu (2x + y^2 + z^2 - 1) + 4p_1 p_2 y z - 2m_F^2 \right) \\
 \beta^{(p_1)} & \equiv 2i \operatorname{Im}(c_s c_p^*) m_F - 2m_\mu \operatorname{Re}(c_s c_p^*) (x + 2y) \\
 \beta^{(p_2)} & \equiv 2i \operatorname{Im}(c_s c_p^*) m_F + 2m_\mu \operatorname{Re}(c_s c_p^*) (x + 2z).
 \end{aligned}$$

$p_1^\sigma$  and  $p_2^\sigma$  can now again be expressed via  $p_+^\sigma$  and  $p_-^\sigma$ . This yields

$$\begin{aligned}
 & \bar{u} \left\{ A \gamma^\sigma - B \left[ (y+z) p_+^\sigma + (z-y) p_-^\sigma \right] + \left[ \alpha \gamma^\sigma + \right. \right. \\
 & \quad \left. \left. + (\beta^{(p_1)} z + \beta^{(p_2)} y) p_+^\sigma + (\beta^{(p_1)} z - \beta^{(p_2)} y) p_-^\sigma \right] \gamma^5 \right\} u
 \end{aligned} \tag{3.1.22}$$

Next, the Gordon decomposition can be applied and every term that does not contribute to the AMM (i.e. is not proportional to  $i\sigma^{\sigma\nu}$ ) can be neglected. We thus obtain the final result for the numerator  $N_{\text{AMM}}^\sigma$  that contributes to the AMM in the scattering amplitude (3.1.1).

$$N_{\text{AMM}}^\sigma = - \left[ (|c_s|^2 + |c_p|^2) m_\mu x + (|c_s|^2 - |c_p|^2) m_F \right] (x-1) \bar{u} \left\{ i \sigma^{\sigma\nu} p_{-\nu} \right\} u \tag{3.1.23}$$

By comparing the contribution of  $N_{\text{AMM}}^\sigma$  with the general form of the AMM contribution given in (2.2.6) gives us

$$-q_F \int \frac{N_{\text{AMM}}^\sigma}{ABC} \frac{d^4\ell}{(2\pi)^4} \stackrel{!}{=} -ie \bar{u} \left\{ i \frac{1}{2m} \sigma^{\sigma\nu} p_{-\nu} F_M(q'^2) \right\} u, \quad (3.1.24)$$

and with the help of the Feynman trick for the denominator an expression for the form factor  $F_M(q'^2)$ :

$$\begin{aligned} F_M(q'^2) &= 4m_\mu \frac{q_F}{e} i \int \frac{d^4\ell}{(2\pi)^4} \iiint_0^1 dx dy dz \delta(x+y+z-1) \times \\ &\quad \times \frac{x(x-1)m_\mu(|c_s|^2 + |c_p|^2) + (x-1)(|c_s|^2 - |c_p|^2)m_F}{(\ell^2 - \Delta + i\epsilon)^3} \\ &\stackrel{(2.3.25)}{=} 4m_\mu \frac{q_F}{e} \frac{1}{32\pi^2} \iiint_0^1 dx dy dz \delta(x+y+z-1) \\ &\quad \times \frac{x(x-1)m_\mu(|c_s|^2 + |c_p|^2) + (x-1)(|c_s|^2 - |c_p|^2)m_F}{\Delta} \end{aligned} \quad (3.1.25)$$

Inserting (3.1.5) with  $q'^2 = 0$  and introducing the abbreviations

$$\Omega_F = \frac{m_F}{m_\mu} \quad \text{and} \quad \Omega_H = \frac{m_H}{m_\mu} \quad (3.1.26)$$

yields

$$\begin{aligned} F_M(0) &= 4m_\mu^2 \frac{q_F}{e} \frac{1}{32\pi^2} \iiint_0^1 dx dy dz \delta(x+y+z-1) \\ &\quad \times \frac{x(x-1)(|c_s|^2 + |c_p|^2) + (x-1)(|c_s|^2 - |c_p|^2)\Omega_F}{m_\mu^2(y^2 + z^2) + 2m_\mu^2 yz + m_H^2 x - (1-x)(m_\mu^2 - m_F^2)} \\ &= -\frac{q_F}{8\pi^2 e} \iiint_0^1 dx dy dz \delta(x+y+z-1) \times \\ &\quad \times \frac{|c_s|^2(1-x)(x + \Omega_F) + |c_p|^2(1-x)(x - \Omega_F)}{(1-x)^2 + \Omega_H^2 x - (1-x)(1 - \Omega_F^2)} \\ &= -\frac{q_F}{8\pi^2 e} \int_0^1 dx \int_0^{1-x} dy \frac{|c_s|^2(1-x)(x + \Omega_F) + |c_p|^2(1-x)(x - \Omega_F)}{(1-x)^2 + \Omega_H^2 x - (1-x)(1 - \Omega_F^2)} \end{aligned} \quad (3.1.27)$$

Executing the integration over  $y$  and substituting  $u$  for  $1-x$  yields the final result for the Fermion-Scalar contribution to the AMM:

$$[a_\mu]_F = -\frac{q_F}{8\pi^2 e} \int_0^1 du \frac{|c_s|^2(1-u + \Omega_F) + |c_p|^2(1-u - \Omega_F)}{u^2 + \Omega_H^2(1-u) + u(\Omega_F^2 - 1)} u^2 \quad (3.1.28)$$

## 3.2 Interaction of a charged scalar with the EM field

In the second topology, the interaction of an internal charged scalar boson  $H$  with a photon of the electromagnetic field, as shown in Fig. 3.2, is considered. The application of the Feynman rules for this diagram yields

$$\begin{aligned} \mathcal{M}^\sigma &= \int \frac{d^4q}{(2\pi)^4} \bar{u}(p_2) i(c_s + c_p \gamma^5) \frac{i(-\not{q} + m_F)}{q^2 - m_F^2 + i\epsilon} i(c_s^* - c_p^* \gamma^5) \frac{i}{k_2^2 - m_H^2 + i\epsilon} \times \\ &\quad \times \frac{i}{k_1^2 - m_H^2 + i\epsilon} u(p_1) \end{aligned} \quad (3.2.1)$$

$$= q_H \int \frac{d^4 q}{(2\pi)^4} \bar{u}(p_2) \frac{(c_s + c_p \gamma^5)(-\not{q} + m_F)(c_s^* - c_p^* \gamma^5)(k_1 + k_2)^\sigma}{(q^2 - m_F^2 + i\varepsilon)(k_2^2 - m_H^2 + i\varepsilon)(k_1^2 - m_H^2 + i\varepsilon)} u(p_1) \quad (3.2.2)$$

$$\equiv q_H \int \frac{N^\sigma}{ABC} \frac{d^4 q}{(2\pi)^4} \quad (3.2.3)$$

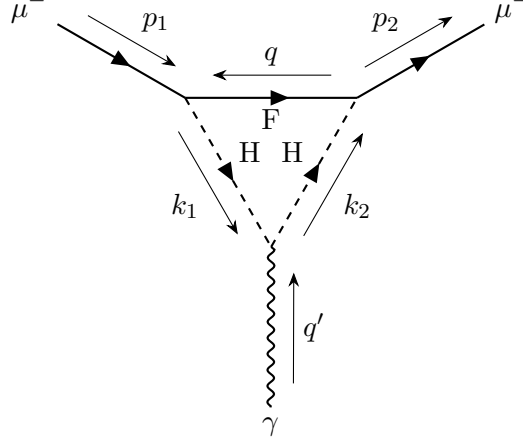


Figure 3.2: Absorption of a photon via the internal Scalar Line

Appendix A.5 shows, that the contribution to the AMM can be determined by evaluating the integral

$$[a_\mu]_S = -\frac{q_H}{8\pi^2 e} \int_0^1 du \frac{|c_s|^2(u + \Omega_F) + |u_p|^2(u - \Omega_F)}{u^2 + \Omega_F^2(1-u) + u(\Omega_H^2 - 1)} (u^2 - u) \quad (3.2.4)$$

## 4 Contributions within the Two-Higgs-Doublet model

The Two-Higgs-Doublet Model (2HDM) extends the SM by introducing a second complex scalar SU(2) doublet and thus enhances the Higgs sector with additional neutral and charged scalars. This simple augmentation not only provides new sources of CP-violation and potential dark-matter candidates, but also alters the pattern of Yukawa interactions and gauge couplings in ways that can address the puzzle of the muon’s anomalous magnetic moment [9]. The following introduction to the model is based on [10].

### 4.1 Introduction to the Two-Higgs-Doublet Model

The SM is extended through the addition of a second SU(2) complex scalar doublet  $\Phi_2$  with hypercharge  $Y = 1/2$ , complementing the original SM Higgs doublet  $\Phi_1$ . Both doublets develop non-zero vacuum expectation values (VEVs)  $\langle \Phi_i \rangle = v_i$ , where  $v$  is assigned to  $\sqrt{v_1^2 + v_2^2} = 246$  GeV. The most general scalar potential in the rotated Higgs basis, which is introduced in the following, is given by [11]:

$$\begin{aligned}
 V = & m_{11}^2(H_1^\dagger H_1) + m_{22}^2(H_2^\dagger H_2) - m_{12}^2(H_1^\dagger H_2 + \text{h.c.}) + \\
 & + \frac{\lambda_1}{2}(H_1^\dagger H_1)^2 + \frac{\lambda_2}{2}(H_2^\dagger H_2)^2 + \lambda_3(H_1^\dagger H_1)(H_2^\dagger H_2) + \\
 & + \lambda_4(H_1^\dagger H_2)(H_2^\dagger H_1) + \left[ \frac{\lambda_5}{2}(H_1^\dagger H_2)^2 + \text{h.c.} \right] + \\
 & + \left[ (\lambda_6(H_1^\dagger H_1) + (\lambda_7(H_2^\dagger H_2))) H_1^\dagger H_2 + \text{h.c.} \right].
 \end{aligned} \tag{4.1.1}$$

As we work in the CP-conserving limit, we take all the parameters  $m_{ij}$  and  $\lambda_i$  to be real. The Higgs basis is now rotated using the angle  $\beta = \tan^{-1}(v_2/v_1)$ .

$$\begin{pmatrix} H_1 \\ H_2 \end{pmatrix} = \begin{pmatrix} \cos \beta & \sin \beta \\ -\sin \beta & \cos \beta \end{pmatrix} \begin{pmatrix} \Phi_1 \\ \Phi_2 \end{pmatrix}. \tag{4.1.2}$$

In this basis, only  $H_1$  contains the SM-like Higgs boson with the aforementioned non-zero VEV, while  $H_2$  has vanishing VEV. The corresponding fields of the new basis can thus be parameterized via

$$H_1 = \frac{1}{\sqrt{2}} \begin{pmatrix} \sqrt{2} G^+ \\ v + H_1^0 + iG^0 \end{pmatrix}, \quad H_2 = \frac{1}{\sqrt{2}} \begin{pmatrix} \sqrt{2} H^+ \\ H_2^0 + iA^0 \end{pmatrix}. \tag{4.1.3}$$

The so-called *Goldstone-Bosons*  $G^+$  and  $G^0$  are “eaten up” by the  $W^\pm$  and  $Z^0$  bosons in the Higgs mechanism within the process of spontaneous electroweak symmetry breaking. The remaining charged scalar  $H^+$  denotes a new physical scalar boson that may be involved in several decay processes which are absent in the SM [12].  $H_{1,2}^0$  and  $A^0$  are the CP-even and CP-odd neutral scalars, whose mass eigenstates are given by [13]:

$$\begin{pmatrix} h \\ H \end{pmatrix} = \begin{pmatrix} \cos(\alpha - \beta) & \sin(\alpha - \beta) \\ -\sin(\alpha - \beta) & \cos(\alpha - \beta) \end{pmatrix} \begin{pmatrix} H_1^0 \\ H_2^0 \end{pmatrix} \tag{4.1.4}$$

with the angle  $\alpha$  being determined via

$$\sin 2(\alpha - \beta) = \frac{2\lambda_6 v^2}{m_H^2 - m_h^2}. \quad (4.1.5)$$

In the alignment limit ( $\alpha \approx \beta$ ), the light scalar  $h \approx H_1^0$  behaves identically to the SM Higgs boson, while  $H \approx H_2^0$  represents a new heavy scalar. The corresponding eigenvalues yield the masses of the physical scalars and are determined by diagonalizing the mass matrix

$$M_{ij}^2 = \frac{\partial^2 V}{\partial \phi_i \partial \phi_j}, \quad \text{with } \phi_i \in \{G^\pm, H^\pm, G^0, H_i^0, A^0\}. \quad (4.1.6)$$

We demonstrate the derivation of the mass matrix exemplarily for the charged bosons in Appendix A.6. The result is given by

$$M_{\text{charged}}^2 = \begin{pmatrix} m_{22}^2 + \frac{1}{2}v^2\lambda_3 & 0 \\ 0 & 0 \end{pmatrix}. \quad (4.1.7)$$

The mass matrix for the neutral scalars  $H_1^0, H_2^0, A^0$  and  $G^0$  is given by [13]:

$$M_{\text{neutral}}^2 = \begin{pmatrix} \lambda_1 v^2 & \text{Re}(\lambda_6)v^2 & -\text{Im}(\lambda_6)v^2 & 0 \\ \text{Re}(\lambda_6)v^2 & m_{22}^2 + \frac{1}{2}v^2(\lambda_3 + \lambda_4 + \text{Re}(\lambda_5)) & -\frac{1}{2}\text{Im}(\lambda_5)v^2 & 0 \\ -\text{Im}(\lambda_6)v^2 & -\frac{1}{2}\text{Im}(\lambda_5)v^2 & m_{22}^2 + \frac{1}{2}v^2(\lambda_3 + \lambda_4 - \text{Re}(\lambda_5)) & 0 \\ 0 & 0 & 0 & 0 \end{pmatrix}.$$

The corresponding eigenvalues denote the respective masses from the particles:

$$\begin{aligned} m_h^2 &= \lambda_1 v^2, \\ m_H^2 &= m_{22}^2 + \frac{v^2}{2}(\lambda_3 + \lambda_4 + \lambda_5), \\ m_A^2 &= m_H^2 - \lambda_5 v^2, \\ m_{H^\pm}^2 &= m_H^2 - \frac{v^2}{2}(\lambda_4 + \lambda_5). \end{aligned} \quad (4.1.8)$$

At the LEP collider, new charged scalar bosons  $H^\pm$  could have been produced in pairs via the process  $e^+e^- \rightarrow Z/\gamma \rightarrow H^+H^-$ . Since LEP reached center of mass energies of up to about  $\sqrt{s} \sim 200$  GeV, such searches were sensitive to charged scalars with masses up to the kinematic threshold of roughly  $m_{H^\pm} \sim \sqrt{s}/2$ . Dedicated analyses of final states with leptons and neutrinos did not reveal any deviations from the Standard Model predictions. As a result, LEP experiments established a lower mass bound of approximately  $H^\pm \geq 100$  GeV, which continues to serve as a robust constraint on charged Higgs bosons in extended scalar sectors.

After introducing the Higgs sector of the model, we can now face the Yukawa sector. The Yukawa coupling matrices  $Y$  and  $\tilde{Y}$  contain the respective coupling constants that mediate interactions between fermions and scalars. The corresponding Lagrangian is given by [14]:

$$-\mathcal{L}_{\text{Yuk}} = \tilde{Y}_{ij} \bar{\ell}_{L,i} H_1 \ell_{R,j} + Y_{ij} \bar{\ell}_{L,i} H_2 \ell_{R,j} + \text{h.c.}, \quad (4.1.9)$$

with the left-handed doublet and right-handed singlet

$$\ell_{\alpha,i} = \begin{cases} (\nu_i, \lambda_i)_L & \text{for } \alpha = L, \\ \lambda_{R,i} & \text{for } \alpha = R, \end{cases} \quad \text{with } i \in \{e^-, \mu^-, \tau^-\}. \quad (4.1.10)$$

The first term only includes the interaction of leptons with non-physical Goldstone modes and with the SM Higgs boson  $h$ . This term is responsible for the leptons to gain mass in

the SM but is no further relevant in this study. All the new scalars introduced by the model are contained in the second Higgs doublet  $H_2$ . Recalling the corresponding parameterization (4.1.3), one obtains the lepton Yukawa couplings for the physical scalars from the Lagrangian

$$\begin{aligned}
 -\mathcal{L}_{\text{Yuk}} &\supset \frac{1}{\sqrt{2}} Y_{ij} (H_2^0 + iA^0) \bar{\lambda}_{L,i} \lambda_{R,j} + Y_{ij} H^+ \bar{\nu}_{L,i} \lambda_{R,j} + \text{h.c.} \\
 &= \frac{1}{\sqrt{2}} Y_{ij} (H_2^0 + iA^0) \lambda_i^\dagger P_L \gamma^0 P_R \lambda_j + Y_{ij} H^+ \nu_i^\dagger P_L \gamma^0 P_R \lambda_j + \text{h.c.} \\
 &= \frac{1}{\sqrt{2}} Y_{ij} (H_2^0 + iA^0) \bar{\lambda}_i P_R \lambda_j + Y_{ij} H^+ \bar{\nu}_i P_R \lambda_j + \text{h.c.}
 \end{aligned} \tag{4.1.11}$$

with the Yukawa coupling matrix

$$Y = \begin{pmatrix} Y_{ee} & Y_{e\mu} & Y_{e\tau} \\ Y_{\mu e} & Y_{\mu\mu} & Y_{\mu\tau} \\ Y_{\tau e} & Y_{\tau\mu} & Y_{\tau\tau} \end{pmatrix} \tag{4.1.12}$$

and the hermitian conjugate<sup>1</sup>

$$\begin{aligned}
 \text{h.c.} &= \left( \frac{1}{\sqrt{2}} Y_{ij} (H_2^0 + iA^0) \bar{\lambda}_{L,i} \lambda_{R,j} + Y_{ij} H^+ \bar{\nu}_{L,i} \lambda_{R,j} \right)^\dagger \\
 &= \frac{1}{\sqrt{2}} Y_{ij} (H_2^0 - iA^0) (\bar{\lambda}_{L,i} \lambda_{R,j})^\dagger + Y_{ij} H^- (\bar{\nu}_{L,i} \lambda_{R,j})^\dagger \\
 &= \frac{1}{\sqrt{2}} Y_{ij} (H_2^0 - iA^0) \lambda_{R,j}^\dagger \gamma^0 \lambda_{L,i} + Y_{ij} H^- \lambda_{R,j}^\dagger \gamma^0 \nu_{L,i} \\
 &= \frac{1}{\sqrt{2}} Y_{ij} (H_2^0 - iA^0) \bar{\lambda}_j P_L \lambda_i + Y_{ij} H^- \bar{\lambda}_j P_L \nu_i.
 \end{aligned} \tag{4.1.13}$$

The term involving the negatively charged scalar arises from the same Feynman diagram as the positively charged scalar, but with reversed momentum. Thus, it does not lead to additional contributions and can be neglected. The final Lagrangian then reads

$$-\mathcal{L}_{\text{Yuk}} \supset \frac{1}{\sqrt{2}} Y_{ij} (H_2^0 + iA^0) \bar{\lambda}_i P_R \lambda_j + Y_{ij} H^+ \bar{\nu}_i P_R \lambda_j + \frac{1}{\sqrt{2}} Y_{ij} (H_2^0 - iA^0) \bar{\lambda}_j P_L \lambda_i. \tag{4.1.14}$$

## 4.2 Analysis of the Impact on muon $g$ -2 by different Yukawa Coupling textures

We will use the results from the previous section to determine the scalar and pseudoscalar coupling constants,  $c_s$  and  $c_p$ , for the distinct coupling textures in dependency of the respective Yukawa coupling  $Y_{ij}$ . These constants will then be substituted into the general formulae (3.1.28) and (3.2.4) to calculate the contributions for the given textures and particles. The Yukawa coupling matrices corresponding to the textures considered are given as

$$\begin{aligned}
 \text{tex. 1 : } Y &= \begin{pmatrix} 0 & 0 & 0 \\ 0 & Y_{\mu\mu} & 0 \\ 0 & 0 & 0 \end{pmatrix}, & \text{tex. 2 : } Y &= \begin{pmatrix} 0 & 0 & 0 \\ 0 & 0 & 0 \\ 0 & Y_{\tau\mu} & 0 \end{pmatrix}, \\
 \text{tex. 3 : } Y &= \begin{pmatrix} 0 & Y_{e\mu} & 0 \\ 0 & 0 & 0 \\ 0 & 0 & 0 \end{pmatrix}, & \text{tex. 4 : } Y &= \begin{pmatrix} 0 & 0 & 0 \\ 0 & 0 & Y_{\mu\tau} \\ 0 & Y_{\tau\mu} & 0 \end{pmatrix}.
 \end{aligned} \tag{4.2.1}$$

<sup>1</sup> The expansion is done with the help of the projection operators, introduced in Appendix A.7.

### 4.2.1 Texture 1: Muon-Muon Coupling

For the first texture, the Lagrangian (4.1.14) reads

$$\begin{aligned}
 -\mathcal{L}_{\text{Yuk}} \supset & \frac{1}{\sqrt{2}} Y_{\mu\mu} (H_2^0 + iA^0) \bar{\mu} \left( \frac{1 + \gamma^5}{2} \right) \mu + Y_{\mu\mu} H^+ \bar{\nu}_\mu \left( \frac{1 + \gamma^5}{2} \right) \mu \\
 & + \frac{1}{\sqrt{2}} Y_{\mu\mu} (H_2^0 - iA^0) \bar{\mu} \left( \frac{1 - \gamma^5}{2} \right) \mu \\
 = & \frac{1}{\sqrt{2}} Y_{\mu\mu} H^0 \bar{\mu} \mu + \frac{i}{\sqrt{2}} Y_{\mu\mu} A^0 \bar{\mu} \gamma^5 \mu + \frac{1}{2} Y_{\mu\mu} H^+ \bar{\nu}_\mu (1 + \gamma^5) \mu
 \end{aligned} \tag{4.2.2}$$

We can now compare this Lagrangian with the general structure (3.0.1) and thus determine the (pseudo-)scalar coupling constants for the respective particles to

$$\begin{aligned}
 c_s^{H^0} &= -\frac{1}{\sqrt{2}} Y_{\mu\mu}, & c_p^{H^0} &= 0, \\
 c_s^{H^+} &= \frac{1}{2} Y_{\mu\mu}, & c_p^{H^+} &= \frac{1}{2} Y_{\mu\mu}, \\
 c_s^{A^0} &= 0, & c_p^{A^0} &= -\frac{i}{\sqrt{2}} Y_{\mu\mu}.
 \end{aligned}$$

These results can be inserted into the formulas (3.1.28) and (3.2.4) from which we obtain

$$\Delta a_\mu^{H^0} = \frac{Y_{\mu\mu}^2}{16\pi^2} \int_0^1 du \frac{u^2(2-u)}{u^2 + \Omega_{H^0}^2(1-u)}, \tag{4.2.3}$$

$$\Delta a_\mu^{A^0} = \frac{Y_{\mu\mu}^2}{16\pi^2} \int_0^1 du \frac{-u^3}{u^2 + \Omega_{A^0}^2(1-u)}, \tag{4.2.4}$$

$$\Delta a_\mu^{H^+} = \frac{Y_{\mu\mu}^2}{16\pi^2} \int_0^1 du \frac{u(u-1)}{u + (\Omega_{H^+}^2 - 1)} \tag{4.2.5}$$

as concrete expressions for the respective contributions. The total contribution by the second Higgs doublet is then given as the sum over the contributions from all additional scalars:

$$\Delta a_\mu = \sum_S \Delta a_\mu^S. \tag{4.2.6}$$

Due to charge conservation, the interaction involving the charged scalar always requires the internal fermion to be neutral. Neutrinos are the only particles in the SM that carry this property and thus the virtual fermion involved in the interaction is a muon neutrino whose mass can be neglected compared to the mass of the muon ( $\Omega_\nu \rightarrow 0$ ). As charge has always to be conserved and the neutrino masses from the other lepton generations can also be neglected, the charged scalar's contribution remains the same in all textures. In the interactions involving the neutral scalars, the charge is carried by the internal muon and thus the denominator in (3.1.28) simplifies to the results given above.

The expressions can be computed using the *scipy.integrate* package in *Python*. The results can be seen in Fig. 4.1a). First, we take a closer look at the irregular behavior of the  $H^+$  contribution in the mass range of the muon mass ( $\sim 0.1$  GeV). The integral diverges here as the integrand has a pole within the integration interval at  $\Omega_{H^+} = 1$ . Therefore, we split the integration into two segments that avoid this pole and observe a sign flip of the contribution beyond the pole. We will now make certain approximations of the expressions (4.2.3) - (4.2.5) to give some justifications for the influences from the neutral scalars on  $g - 2$ . For lower masses ( $\Omega_S \ll 1$ ), the integrands reduce to fundamental polynomials which can be evaluated to  $3/2$ ,  $-1/2$  and  $1/2$ , respectively. The contribution is therefore constant with respect to the scalar masses. The limit for higher masses is less obvious and needs a mathematically

demonstrated reasoning. For  $\Omega_{H^+} \gg 1$ , the denominator of (4.2.5) can be approximated via  $\Omega_{H^+}^2$  which can be factored out of the integral and leaves us with the integration

$$\Delta a_{\mu}^{H^+} = \frac{Y_{\mu\mu}^2}{16\pi^2} \frac{1}{\Omega_{H^+}^2} \int_0^1 du u(u-1) = -\frac{1}{6} \frac{Y_{\mu\mu}^2}{16\pi^2} \frac{1}{\Omega_{H^+}^2} \quad (4.2.7)$$

This result does not only explain the global form of the curve<sup>2</sup> but also explains the sign flip of the contribution. The approximation of the neutral scalars is done by similar considerations. However, we only present the approximation for the CP-odd scalar  $A^0$  in particular, because the other case is achieved equivalently. For  $\Omega_{A^0} \gg 1$ , the squared term in the denominator can be neglected over the whole integration interval, except for  $z \rightarrow 1$ . We are thus left with

$$\Delta a_{\mu}^{A^0} \approx -\frac{Y_{\mu\mu}^2}{16\pi^2} \int_0^1 du \frac{u^3}{1 + \Omega_{A^0}^2(1-u)}. \quad (4.2.8)$$

Introducing the substitution  $x := 1 + \Omega_{\phi^0}^2(1-u)$  gives

$$\Delta a_{\mu}^{A^0} \approx \frac{Y_{\mu\mu}^2}{16\pi^2} \frac{1}{\Omega_{A^0}^8} \int_{1+\Omega_{A^0}^2}^1 dx \frac{(1 + \Omega_{A^0}^2 - x)^3}{x} \approx \frac{Y_{\mu\mu}^2}{16\pi^2} \frac{1}{\Omega_{A^0}^2} \ln x \Big|_{1+\Omega_{A^0}^2}^1 \approx -\frac{Y_{\mu\mu}^2}{8\pi^2} \frac{1}{\Omega_{A^0}^2} \ln \Omega_{A^0}. \quad (4.2.9)$$

On a double-logarithmic scale, this gives exactly the behavior we can see in the contributions from both the  $A^0$  particle. Furthermore, we can see that in higher mass regions, only  $H^0$  contributes positively to the  $g-2$  whereas the CP-odd and charged scalar contribute negatively. If we compare the predicted contributions with the experimentally demanded value (shaded in gray), we can claim that the CP-even scalar dominates the contribution and thus forces the mass hierarchy of the particles to be  $m_{H^0} = m_{A^0, H^+} - \Delta m$ . This is what we already stated earlier in section 4.1.

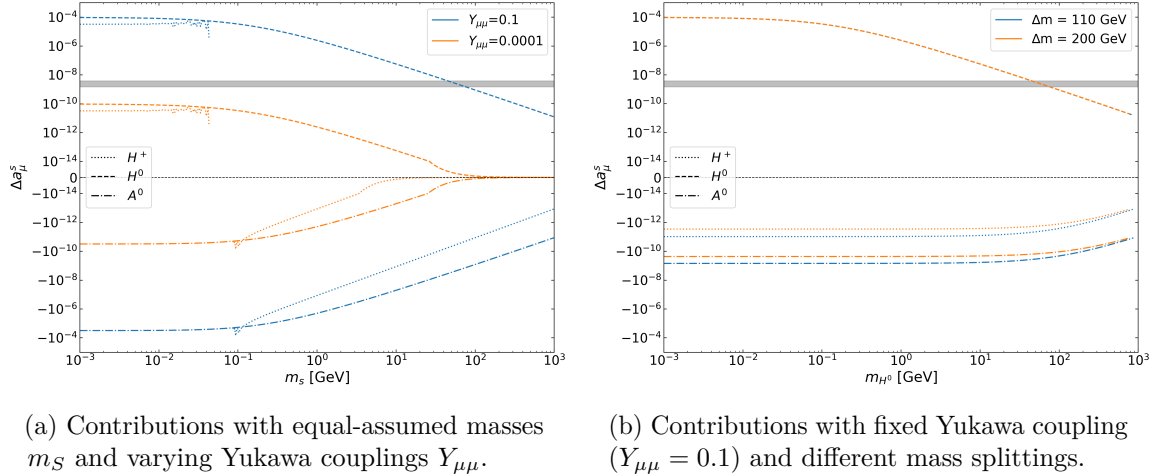


Figure 4.1: Comparison of the contributions from the respective scalars to  $\Delta a_{\mu}$  in coupling texture 1. In (a), equal masses were assumed to determine the magnitude of the respective contributions. In (b), we fixed the Yukawa coupling and show how different mass splittings influence the distinct contributions of the particles. The gray area denotes the experimentally found  $2\sigma$ -region of  $\Delta a_{\mu}$ .

Fig. 4.1b) shows that this mass hierarchy significantly suppresses the negative influences of the new particles and thus achieves our requirements. Moreover, it can be seen that in higher mass

<sup>2</sup> You can plot  $-1/x^2$  with logarithmic scales to see that the curve fits the graph shown in 4.1.

regions, the influences of the scalars converge into the same order of magnitude. Hence, for a fixed Yukawa coupling of around  $Y_{\mu\mu} = 0.1$  our model achieved to predict an upper bound for the CP-even scalar ( $\sim \mathcal{O}(10) - \mathcal{O}(100)$  GeV). However, different Yukawa couplings are possible. Therefore, we have to run a parameter space scan to determine which combinations of Yukawa couplings and CP-even scalar masses are allowed to fit into the  $1\sigma$  and  $2\sigma$  region of the experimentally found value for  $\Delta a_\mu$ . A total number of 40,000 different pairs was tested. The resulting parameter space that is consistent with experiment is indicated in Fig. 4.2. As you can see, the decreasing contribution by higher scalar masses is compensated by increasing Yukawa couplings. We also shaded regions of the parameter space that are either already ruled out by experiments or lie within a range that upcoming experiments can probe and potentially confirm or exclude. Via its loop-induced two-photon coupling,  $H^0$  can be produced in electron beam dumps and in supernova cores and be long-lived below the muon threshold. E137 has not yet observed such decays and therefore restricts the parameter space in the low mass region (green shaded). The pink shaded bounds from SN1987A arise because the long-living scalars  $H^0$  could have carried away lots of the supernova's energy, leading to an excessive cooling of the core, which was not seen. BaBar's vain search for the decay  $e^+e^- \rightarrow \mu^+\mu^-Z'$ ,  $Z' \rightarrow \mu^+\mu^-$  excludes the blue region and the dashed Belle-II line shows the much stronger reach expected with a hundred times more data. Finally,  $Z \rightarrow \mu^+\mu^-H^0$  would produce a  $Z \rightarrow 4\mu$  signature which CMS has not yet observed and hence constraints the parameter space within the purple bounds.

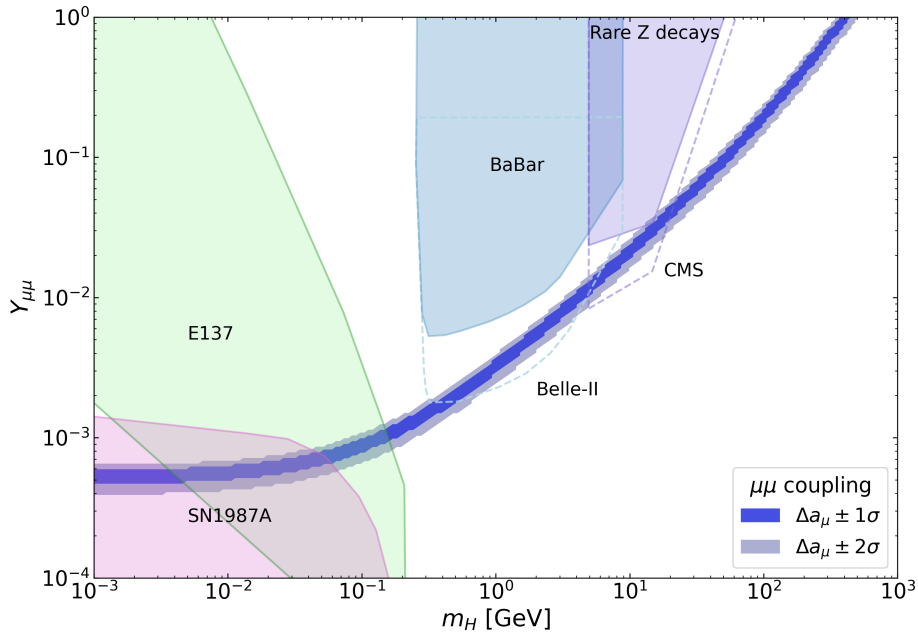


Figure 4.2: Allowed Parameter Space for  $Y_{\mu\mu}$  and  $m_{H^0}$  to match the  $1\sigma$  and  $2\sigma$  ranges of  $\Delta a_\mu$ . The contribution was computed with the sum of (4.2.3) - (4.2.5), considering the mass hierarchy  $m_{H^0} = m_{H^+,A^0} - \Delta m$ . The plot also includes those (shaded) regions that are already experimentally investigated and excluded by Supernovae 1987A ([15], [16]), E137 [17], BaBar [18] and CMS [19]. The dashed lines indicate constraints that may be achieved by future experiments at Belle-II [20]. The processed and illustrated data from SN1987A, E138 and CMS is given in [21], whereas BaBar can be found in [10].

### 4.2.2 Texture 2 & 3: Tauon-Muon and Electron-Muon Coupling

Contrary to the previous section, the muon now couples with a lepton from another generation in the SM. Consequently, we now turn to the off-diagonal Yukawa couplings  $Y_{e\mu}$  and  $Y_{\tau\mu}$ , which couple the muon to the electron and tauon fields, respectively, along with the associated scalar fields. The two textures can be dealt with simultaneously as they only distinguish in their respective internal fermion masses and neutrinos. We therefore introduce  $\ell = \tau, e$  for abbreviation. Recalling the Lagrangian of the lepton-specific 2HDM (4.1.14), we can determine the Lagrangian for this scenario to

$$-\mathcal{L}_{\text{Yuk}} \supset \frac{1}{\sqrt{2}} Y_{\ell\mu} (H^0 + iA^0) \bar{\ell} P_R \mu + Y_{\ell\mu} H^+ \bar{\nu}_\ell P_R \mu + \frac{1}{\sqrt{2}} Y_{\ell\mu} (H_2^0 - iA^0) \bar{\mu} P_L \ell \quad (4.2.10)$$

Comparing this result with the general structure of the Lagrangian (3.0.1) furnishes the (pseudo-)scalar coefficients  $c_p$  and  $c_s$ , corresponding to the scalar bosons:

$$\begin{aligned} c_s^{H^+} &= c_p^{H^+} = \frac{1}{2} Y_{\ell\mu} \\ c_s^{H^0} &= -c_p^{H^0} = \frac{i}{2\sqrt{2}} Y_{\ell\mu} \\ c_s^{A^0} &= -c_p^{A^0} = -\frac{1}{2\sqrt{2}} Y_{\ell\mu} \end{aligned}$$

Combined with the derived formula (3.1.28) we obtain the respective contributions:

$$\Delta a_\mu^{\phi^0} = \frac{Y_{\ell\mu}^2}{32\pi^2} \int_0^1 du \frac{u^2(1-u)}{u^2 + \Omega_{\phi^0}^2(1-u) + u(\Omega_\ell^2 - 1)}, \quad \text{with } \phi^0 \in \{H^0, A^0\}. \quad (4.2.11)$$

As mentioned earlier, the charged scalars contribution is identical for all four coupling textures, apart from replacing the coupling constant (in this case with  $Y_{\ell\mu}$ ). Therefore, we refer to (4.2.5) here.

Similarly to texture 1, the contributions from the charge(-less) scalars in the  $\tau - \mu$ - and the  $e - \mu$ - texture are plotted in Fig. 4.3a) and 4.3b). The graphs show exactly the behavior that we expect from the formulae (4.2.5) and (4.2.11): First, it is evident that a three order of magnitude suppression in the Yukawa couplings results in a six order of magnitude reduction of the charged Higgs contribution. This results from the dependency of the squared coupling constant in (4.2.5). The behavior of the contribution by the neutral scalars on the other hand needs some reasoned approximations in upper and lower mass limits for both the leptons and the scalars. Starting point is eq. (4.2.11) for the  $\tau - \mu$ -coupling ( $\Omega_\tau \gg 1$ ). Assuming the lower mass limit for the boson ( $\Omega_{\phi^0} \ll 1$ ), the contribution is a positive constant with respect to  $m_{\phi^0}$ :

$$\Delta a_\mu^{\phi^0} \approx \frac{Y_{\tau\mu}^2}{32\pi^2} \int_0^1 du \frac{u^2(1-u)}{\Omega_\tau^2 u} = \frac{Y_{\tau\mu}^2}{32\pi^2} \frac{1}{6\Omega_\tau}, \quad \text{for } \Omega_\tau \gg \Omega_{\phi^0}, 1. \quad (4.2.12)$$

As soon as the bosonic mass fraction overcomes the tauon mass fraction ( $\mathcal{O}(\Omega_{\phi^0}) \geq \mathcal{O}(\Omega_\tau)$ ), the denominator can be estimated with  $\Omega_{\phi^0}$  and the contribution reads

$$\Delta a_\mu^{\phi^0} \approx \frac{Y_{\tau\mu}^2}{32\pi^2} \frac{1}{\Omega_{\phi^0}^2} \int_0^1 u^2 du = \frac{Y_{\tau\mu}^2}{32\pi^2} \frac{1}{3\Omega_{\phi^0}^2}. \quad (4.2.13)$$

Hence, the behavior matches that of the charged scalar contribution in the high-mass region (cf. (4.2.7)).

We can now consider the  $e - \mu$ -coupling ( $\Omega_e \ll 1$ ). For the lower mass limit of the scalars ( $\Omega_{\phi^0} \ll 1$ ), the integrand simplifies to  $-u$ , which yields  $-1/2$  in the regarded integration interval. The high-mass limit was already discussed in (4.2.13) as this corresponds to  $\Omega_{\phi^0} \gg 1, \Omega_e$ .

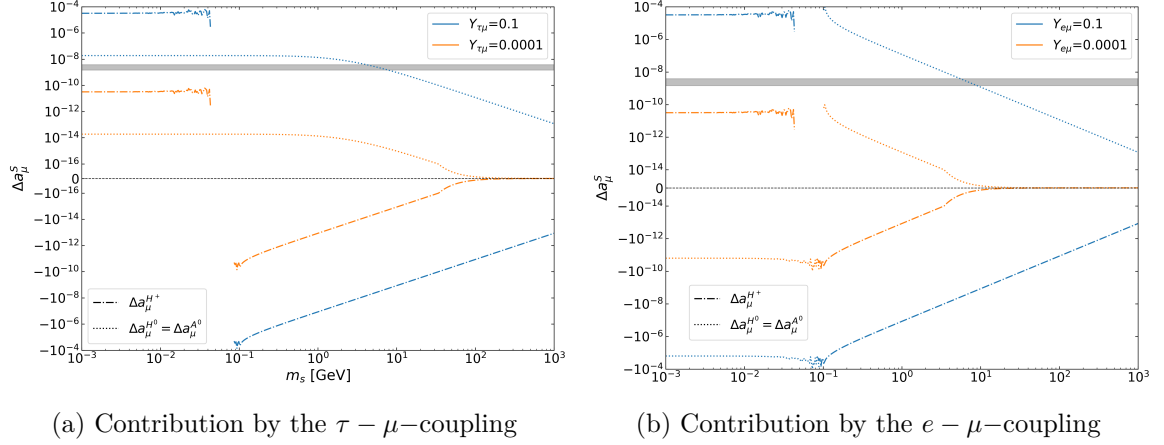


Figure 4.3: Comparison of the contributions from the respective scalars to  $\Delta a_\mu$  in coupling texture 2 (a) and texture 3 (b).

We proceed with the parameter space scan corresponding to the several textures. As before, a mass hierarchy of  $m_{H^0} = m_{H^+/A^0} - 110$  GeV is chosen, in acceptance with the considerations in Section 4.1. Fig. 4.4a) shows both the theoretically allowed pairs of Yukawa couplings  $Y_{\tau\mu}$  and  $Y_{e\mu}$  and the CP-even scalar masses  $m_{H^0}$  as well as the experimentally demanded constraints from ARGUS [22], LEP [23], CMS ([24], [25]). Furthermore, we plotted the curve in the parameter space that denotes the possible pairs of Yukawa couplings  $Y_{e\mu}$  and scalar masses  $m_S$  which make the additional interactions and contributions from the scalars consistent with the SM predicted and experimentally found value of the electronic magnetic moment  $\Delta a_e$ . The function used to compute this contour reads

$$Y_{e\mu}(m_S) = \sqrt{\frac{\Delta a_e^{\text{exp}}}{f_{H^0}(m_S) + f_{A^0}(m_S) + f_{H^+}(m_S)}}, \quad (4.2.14)$$

where

$$f_{\phi^0}(m_S) = \frac{1}{32\pi^2} \int_0^1 du \frac{u^2(1-u)}{u^2 + \Lambda_{\phi^0}(1-u) + u(\Lambda_\mu - 1)} \quad (4.2.15)$$

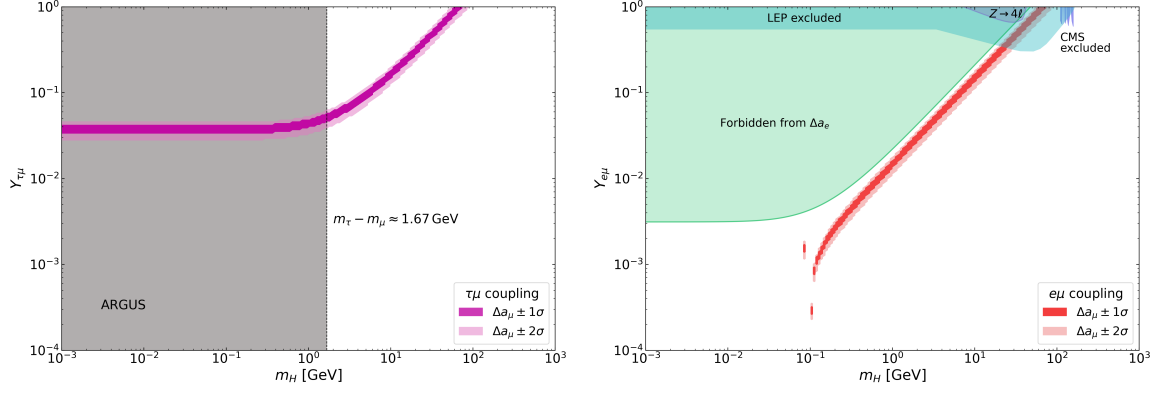
$$f_{H^+}(m_S) = \frac{1}{32\pi^2} \int_0^1 du \frac{u^2 - u}{u + \Lambda_{H^+} - 1}.$$

result from the general one-loop contribution formulae (3.1.28) and (3.2.4), which can be derived in exact the same way for the electron scattering process. Analogously to muonic AMM, we introduced the mass ratios as

$$\Lambda_S = \frac{m_S}{m_e} \quad \text{and} \quad \Lambda_\mu = \frac{m_\mu}{m_e}. \quad (4.2.16)$$

The constraint of the parameter space can be compared to the results from [26], whereas the experimental data for  $\Delta a_e$  was taken from [27].

Regarding the global behavior of both textures it stands out that the parameter space of the  $e - \mu$ -coupling is restricted to scalar masses  $m_{H^0} \geq m_\mu$ . This can be understood by recalling the approximations above ( $\Omega_{\phi^0}, \Omega_e \ll 1$ ). The contribution could be computed to be negative in this case, which would even increase the anomaly in  $g - 2$ . Therefore, only scalar masses  $m_{H^0} \geq m_\mu$  qualify for this texture.



(a)  $Y_{\tau\mu}$  - coupling.

The ARGUS experiment did not observe a  $\tau \rightarrow \mu H$  decay and therefore excludes the mass region  $m_{H^0} < m_{\tau} - m_{\mu}$  [22].

(b)  $Y_{e\mu}$  - coupling.

LEP [23], CMS ([24], [25]) restrict the parameter space due to observations of the  $e^+e^- \rightarrow \mu^+\mu^-$  and the  $Z \rightarrow 4\ell$  decay.

Figure 4.4: Allowed Parameter Space for (a)  $Y_{\tau\mu}$ , (b)  $Y_{e\mu}$  and  $m_{H^0}$  to match the  $1\sigma$  and  $2\sigma$  ranges of  $\Delta a_{\mu}$ . The contribution was computed with the sum of (4.2.5) and (4.2.11) for  $\ell = \tau, e$ , considering the mass hierarchy  $m_{H^0} = m_{H^{+,A^0}} - \Delta m$ . The processed data for (b) is given in [28].

### 4.2.3 Texture 4: Muon - Tauon / Tauon - Muon Coupling

The final Yukawa texture we consider for its effect on  $g - 2$  is the one in which the tau-muon interaction is governed by two nonzero Yukawa entries,  $Y_{\tau\mu}$  and  $Y_{\mu\tau}$ . With (4.1.14), the overall Lagrangian for this scenario reads

$$\begin{aligned}
 -\mathcal{L}_{\text{Yuk}} \supset & \frac{1}{\sqrt{2}} Y_{\tau\mu} (H^0 + iA^0) \bar{\tau} P_R \mu + Y_{\tau\mu} H^+ \bar{\nu}_{\tau} P_R \mu + \frac{1}{\sqrt{2}} Y_{\tau\mu} (H^0 - iA^0) \bar{\mu} P_L \tau \\
 & + \frac{1}{\sqrt{2}} Y_{\mu\tau} (H^0 + iA^0) \bar{\mu} P_R \tau + Y_{\mu\tau} H^+ \bar{\nu}_{\mu} P_R \tau + \frac{1}{\sqrt{2}} Y_{\mu\tau} (H^0 - iA^0) \bar{\tau} P_L \mu
 \end{aligned} \quad (4.2.17)$$

Comparing this Lagrangian with the general form (3.0.1), we once again obtain the (pseudo-) scalar coefficients  $c_p$  and  $c_s$ :

$$\begin{aligned}
 c_s^{H^0} &= \frac{1}{2\sqrt{2}} (Y_{\tau\mu} + Y_{\mu\tau}) & c_p^{H^0} &= \frac{1}{2\sqrt{2}} (Y_{\mu\tau} - Y_{\tau\mu}) \\
 c_s^{H^+} &= \frac{1}{2} Y_{\tau\mu} & c_p^{H^+} &= \frac{1}{2} Y_{\tau\mu} \\
 c_s^{A^0} &= \frac{i}{2\sqrt{2}} (Y_{\mu\tau} - Y_{\tau\mu}) & c_p^{A^0} &= \frac{i}{2\sqrt{2}} (Y_{\tau\mu} + Y_{\mu\tau})
 \end{aligned}$$

The formulae for the computation of the respective contributions are again obtained by inserting the coefficients into the general formulae (3.1.28) and (3.2.4). We thus receive

$$\begin{aligned}
 \Delta a_{\mu}^{\phi^0} &\approx \frac{\Omega_{\tau}}{8\pi^2} \int_0^1 du \frac{u^2 (|c_s|^2 - |c_p|^2)}{u^2 + \Omega_{\phi^0}^2 (1-u) + (\Omega_{\tau}^2 - 1)u} \\
 &= \pm \frac{\Omega_{\tau}}{16\pi^2} Y_{\tau\mu} Y_{\mu\tau} \int_0^1 du \frac{u^2}{u^2 + \Omega_{\phi^0}^2 (1-u) + u(\Omega_{\tau}^2 - 1)}
 \end{aligned} \quad (4.2.18)$$

for the neutral scalars  $H^0$  and  $A^0$  and (again equivalently to (4.2.5))

$$\Delta a_{\mu}^{H^+} = \frac{Y_{\tau\mu}^2}{16\pi^2} \int_0^1 \frac{u^2 - u}{u + \Omega_{H^+}^2 - 1} \quad (4.2.19)$$

for the charged scalar  $H^+$ . In (4.2.18), we used that the muon mass is significantly smaller than the tauon mass, which results in  $\Omega_\tau \gg 1$  and therefore in an approximation of the numerator reading

$$u^2(|c_s|^2(1-u+\Omega_\tau) + |c_p|^2(1-u-\Omega_\tau)) \approx \Omega_\tau u^2(|c_s| - |c_p|). \quad (4.2.20)$$

We can predict the global behavior of the curve by recalling the reasoning from section 4.2.1. For lower masses ( $\Omega_{\phi^0} \ll 1$ ) the integrand simplifies to  $u/\Omega_\tau^2$  which leads to a constant behavior of  $\Delta a_\mu$  with respect to  $m_S$ . For higher masses ( $\Omega_{\phi^0} \gg 1, \Omega_\tau$ ), the same procedure that was used in 4.2.1 can be applied to simplify the integral in (4.2.18) and thus we obtain an analogue result:

$$\lim_{m_{\phi^0} \rightarrow \infty} \Delta a_\mu^{\phi^0} = \pm \frac{\Omega_\tau}{8\pi^2} Y_{\mu\tau} Y_{\tau\mu} \frac{\ln \Omega_{\phi^0}}{\Omega_{\phi^0}^2}. \quad (4.2.21)$$

Overall, we can conclude that the respective contributions should look the same as in the  $\mu - \mu$ -texture which we discussed in 4.2.1. This expectation is verified by the computed results, shown in Fig. 4.5.

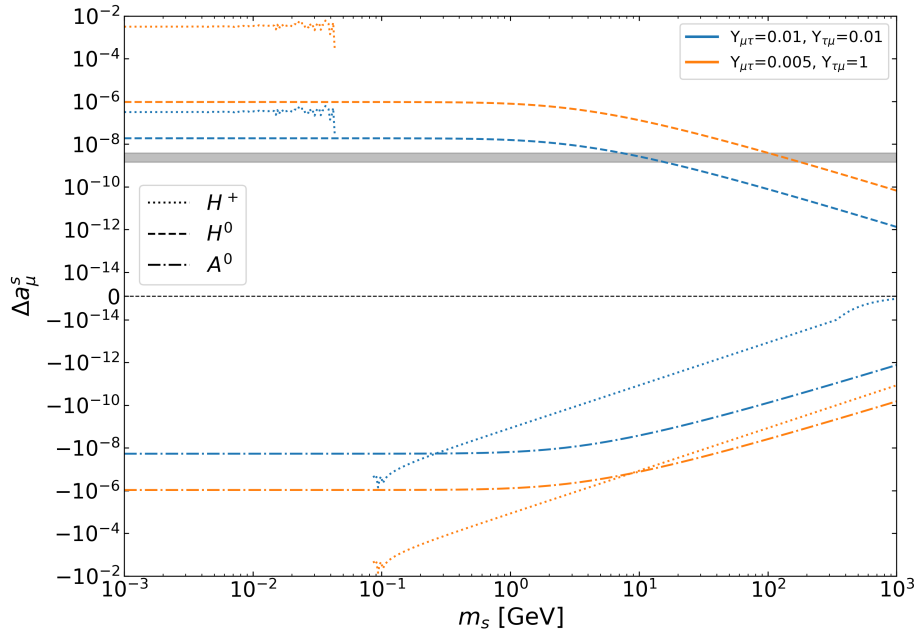


Figure 4.5: Comparison of the contributions from the respective scalars to  $\Delta a_\mu$  in coupling texture 4.

It is important to mention that a mass hierarchy  $m_{H^0} < m_{A^0}$  is crucial at this point as the contributions would otherwise cancel each other out. This is also done because the contribution from the charged scalar has to be suppressed as well and the only possible option besides the choice of an increased mass  $m_{H^+} > m_{H^0}$  would be to lower the value of the Yukawa coupling  $Y_{\tau\mu}$ . This, on the other hand, would force the coupling constant  $Y_{\mu\tau}$  to be increased in order to keep  $\sqrt{Y_{\mu\tau} Y_{\tau\mu}}$  constant. This leads to a problem as soon as  $Y_{\mu\tau} \gg 1$  because then we cannot neglect the higher-order contributions in the loop anymore and our formulae (3.2.4) and (3.1.28) would not yield proper results anymore.

The parameter space belonging to the final texture is given in Fig. 4.6. Equally to texture 2, we indicated the region that was excluded by ARGUS experiment which did not observe the  $\tau \rightarrow \mu H$  decay.

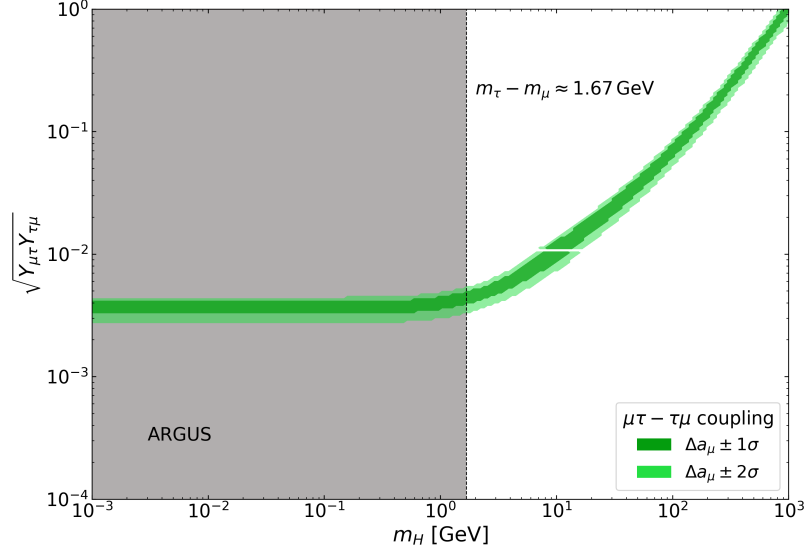


Figure 4.6: Allowed Parameter Space for  $\sqrt{Y_{\tau\mu}Y_{\mu\tau}}$  and  $m_{H^0}$  to match the  $1\sigma$  and  $2\sigma$  ranges of  $\Delta a_\mu$ . The contribution was again computed using the sum of (4.2.18) and (4.2.19).

#### 4.2.4 Comparison of Parameter spaces from the distinct textures

To finalize our analysis of the impact on  $g - 2$  by different coupling scenarios of new Higgs scalars and different lepton generations, we compare all the four parameter spaces in Fig. 4.7.

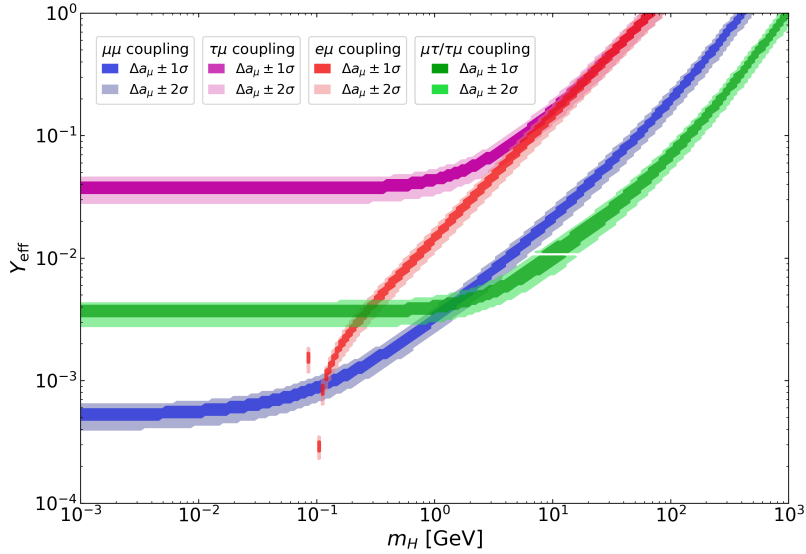


Figure 4.7: Comparison of the allowed parameter spaces, corresponding to the respective coupling textures.  $Y_{\text{eff}}$  indicates  $Y_{\ell\mu}$ , with  $\ell \in \{e, \mu, \tau\}$  for texture 1 - 3 and  $\sqrt{Y_{\tau\mu}Y_{\mu\tau}}$  for texture 4.

The plot shows how the effective Yukawa coupling  $Y_{\text{eff}}$  required to reproduce  $\Delta a_\mu$  evolves with the scalar mass  $m_{H^0}$  for the four texture choices. In the lower mass regions ( $m_{H^0} \lesssim 10^{-1}$  GeV) the textures separate into a clear hierarchy: the flavor-diagonal  $\mu - \mu$ - texture requires the smallest couplings (down to  $\mathcal{O}(10^{-4})$ ), the mixed  $\mu - \tau / \tau - \mu$  texture occupies an intermediate band, and the purely off-diagonal  $\tau - \mu$ - texture sits systematically higher (few  $10^{-2}$  and above). The  $e - \mu$ - texture starts comparably small at the very light end but rises

earlier with  $m_{H^0}$  and crosses the  $\mu - \mu^-$  and  $\mu\tau/\tau\mu^-$  bands around  $m_{H^0} \sim 0.1 - 1 \text{ GeV}$ , so for intermediate masses its required coupling becomes larger. The  $\mu - \mu^-$ -band on the other hand overcomes the  $\mu\tau/\tau\mu^-$ -texture at  $m_{H^0} \sim \mathcal{O}(1)$ . For  $m_{H^0} \gtrsim 1 \text{ GeV}$  all curves trend upward: heavier scalars demand substantially larger Yukawa couplings to produce the same  $\Delta a_\mu$ . By the higher GeV-TeV scale the required  $Y_{\text{eff}}$  approaches  $\mathcal{O}(1)$ . The vertical positions and crossing points quantify where one texture becomes more or less favorable than another. In particular, the plateau behavior of some textures at very low mass indicates a region where the contribution is relatively mass-insensitive, whereas the steep rise at larger  $m_{H^0}$  reflects the power-suppressed decoupling of heavy scalars. These features suffice to identify the mass ranges where each texture is most economical in coupling strength and to read off the approximate coupling magnitudes needed.

## 5 Conclusion

In this thesis we investigated the anomalous magnetic moment of the muon as a precision probe of physics beyond the Standard Model. Starting from the relativistic Dirac equation we reproduced the tree-level prediction  $g - 2$  and demonstrated how loop corrections in QED generate the leading-order deviation  $\alpha/(2\pi)$ . This provided the theoretical basis and formalism for extracting the anomalous magnetic moment from loop-induced contributions during the scattering process of a muon with an electromagnetic field.

We then derived general one-loop contributions to  $a_\mu$  arising from interactions of the muon with internal charged scalars and fermions coupled to the electromagnetic field. Employing Feynman parameterization, compact expressions for the magnetic form factor  $F_M(q')$  were obtained, allowing us to emphasize the dependence of the correction on the internal particle masses and couplings constants.

Finally, these results were applied to scalar extensions of the SM, focusing on the Two-Higgs-Doublet Model (2HDM). We studied several Yukawa coupling textures and analyzed the parameter dependence of the scalar contributions to the muon AMM. Our results demonstrate that additional scalar states can provide extensive corrections, and that specific parameter regions in masscoupling space are capable of producing contributions of the same order of magnitude as the observed discrepancy between experiment and the SM prediction.

The analysis presented here illustrates how relatively minimal extensions of the SM scalar sector can address one of the most persistent anomalies in particle physics. At the same time, it emphasizes the sensitivity of  $a_\mu$  to details of the Yukawa sector, underscoring the importance of continued precision studies.

Looking forward, further progress on both experimental and theoretical fronts will be decisive. The ongoing Muon  $g - 2$  Collaboration will sharpen the experimental determination of  $a_\mu$  while forthcoming lattice QCD calculations aim to reduce the dominant hadronic uncertainties in the SM prediction. In parallel, extending the analysis of this work to other classes of BSM models could provide additional feasible explanations or further constrain the space of possible new interactions.

# Appendix

## A.1 Gamma matrices: Formulas and identities

The  $\gamma$ - (or Dirac-) matrices result from the ansatz to linearize the Klein-Gordon-Equation and are introduced in Section 2.1. This section provides an overview about the most relevant identities and formulas that are used throughout various calculations in this thesis.

- (Anti-)Commutation Relations:

$$\{\gamma^\mu, \gamma^\nu\} = 2g^{\mu\nu} \quad \text{and} \quad [\gamma^\mu, \gamma^\nu] = -2i\sigma^{\mu\nu} \quad (\text{A.1.1})$$

- Miscellaneous  $\gamma$ -product identities<sup>1</sup>

$$\begin{aligned} \gamma^\mu \gamma_\mu &= 4 \\ \gamma^\mu \gamma^\nu \gamma_\mu &= -2\gamma^\nu \\ \gamma^\mu \gamma^\nu \gamma^\sigma \gamma_\mu &= 4g^{\nu\sigma} \\ \gamma^\mu \gamma^\nu \gamma^\rho \gamma^\sigma \gamma_\mu &= -2\gamma^\sigma \gamma^\rho \gamma^\nu \\ \gamma^\mu \gamma^\sigma \gamma^\nu &= 2(g^{\sigma\nu} \gamma^\mu - g^{\mu\nu} \gamma^\sigma + g^{\mu\sigma} \gamma^\nu) - \gamma^\nu \gamma^\sigma \gamma^\mu \end{aligned} \quad (\text{A.1.2})$$

- The  $\gamma^5$ -matrix is defined as

$$\gamma^5 = i\gamma^0 \gamma^1 \gamma^2 \gamma^3. \quad (\text{A.1.3})$$

and it fulfills

$$\gamma^5 \gamma^5 = \mathbf{1} \quad \text{and} \quad \{\gamma^5, \gamma^\sigma\} = 0. \quad (\text{A.1.4})$$

## A.2 Gordon decomposition

The Gordon decomposition is used repeatedly in this thesis: after computing the invariant scattering amplitude  $M^\sigma$  it rewrites the Dirac bilinears into the vector and Pauli (tensor) structures so that the electromagnetic form factors can be identified directly from the result. The Gordon identity is given as

$$\bar{u}(p_2) \gamma^\sigma u(p_1) = \frac{1}{2m} \bar{u}(p_2) \left[ (p_1 + p_2)^\sigma + i \sigma^{\sigma\nu} (p_1 - p_2)_\nu \right] u(p_1). \quad (\text{A.2.1})$$

First, we recall the (anti-)commutator relations of the  $\gamma$ -matrices:

$$\{\gamma^\sigma, \gamma^\nu\} = 2g^{\sigma\nu} \quad \text{and} \quad [\gamma^\sigma, \gamma^\nu] = -2i \sigma^{\sigma\nu}. \quad (\text{A.2.2})$$

Thus, we can write  $i\sigma^{\sigma\nu}$  in terms of two equivalent expressions:

$$\begin{aligned} i\sigma^{\sigma\nu} &= -\frac{1}{2}(\gamma^\sigma \gamma^\nu - \gamma^\nu \gamma^\sigma) \\ &= -\frac{1}{2}(\gamma^\sigma \gamma^\nu - (2g^{\sigma\nu} - \gamma^\sigma \gamma^\nu)) \\ &= g^{\sigma\nu} - \gamma^\sigma \gamma^\nu \end{aligned} \quad (\text{A.2.3})$$

$$\begin{aligned} i\sigma^{\sigma\nu} &= -\frac{1}{2}(\gamma^\sigma \gamma^\nu - \gamma^\nu \gamma^\sigma) \\ &= -\frac{1}{2}(2g^{\sigma\nu} - 2\gamma^\nu \gamma^\sigma) \\ &= \gamma^\nu \gamma^\sigma - g^{\sigma\nu} \end{aligned} \quad (\text{A.2.4})$$

with which we obtain

---

<sup>1</sup> Those relations follow directly from (A.1.1).

$$\begin{aligned}
i \sigma^{\sigma\nu} (p_1 - p_2)_\nu &= (\gamma^\nu \gamma^\sigma - g^{\sigma\nu}) p_{1,\nu} - (g^{\sigma\nu} - \gamma^\sigma \gamma^\nu) p_{2,\nu} \\
&= \gamma^\nu \gamma^\sigma p_{1,\nu} - p_1^\sigma - p_2^\sigma + \gamma^\sigma \gamma^\nu p_{2,\nu} \\
&= \gamma^\sigma \not{p}_1 - p_1^\sigma - p_2^\sigma + \not{p}_2 \gamma^\sigma
\end{aligned} \tag{A.2.5}$$

Now, we rearrange (A.2.1) and make use of the Dirac equation (2.1.16):

$$\begin{aligned}
\bar{u}(p_2) [i \sigma^{\sigma\nu} (p_1 - p_2)_\nu] u(p_1) &= \bar{u}(p_2) [2m \gamma^\sigma - (p_1 + p_2)^\sigma] u(p_1) \\
&= \bar{u}(p_2) [\not{p}_2 \gamma^\sigma - (p_1 + p_2)^\sigma + \gamma^\sigma \not{p}_1] u(p_1)
\end{aligned} \tag{A.2.6}$$

which is similar to the expression in (A.2.5). A similar identity can be proven for  $\gamma^5$ -matrices involved:

$$\bar{u}(p_2) \{ (p_1^\sigma + p_2^\sigma) \gamma^5 \} u(p_1) = \bar{u}(p_2) \{ i \sigma^{\sigma\nu} (p_{1\nu} - p_{2\nu}) \gamma^5 \} u(p_1) \tag{A.2.7}$$

### A.3 Feynman rules

Feynman diagrams offer a visual shorthand for the intricate math of quantum field theory. In this section we present the Feynman rules that translate specific diagram elements into the expressions used in this thesis. They are taken from [7], pp. 115ff.

Incoming and outgoing particles are pictured by external lines. They correspond to four component Dirac spinors for fermions or polarization vectors for photons:

$$\begin{aligned}
\text{Incoming fermion: } \begin{array}{c} p \\ \longrightarrow \\ \bullet \end{array} &= u(p); & \text{Incoming photon: } \begin{array}{c} p \\ \longrightarrow \\ \bullet \end{array} &= \epsilon_\sigma(p) \\
\text{Outgoing fermion: } \begin{array}{c} p \\ \longrightarrow \\ \bullet \end{array} &= \bar{u}(p); & \text{Outgoing photon: } \begin{array}{c} p \\ \longrightarrow \\ \bullet \end{array} &= \epsilon_\sigma^*(p)
\end{aligned}$$

The internal lines that correspond to virtual particles within the interaction blob (shown in Fig. 2.1) are called propagators and represent the following:

$$\begin{aligned}
\text{Spin 0 boson: } \begin{array}{c} p \\ \longrightarrow \\ \bullet \text{---} \bullet \end{array} &= \frac{i}{p^2 - m^2} \\
\text{Spin } \frac{1}{2} \text{ fermion: } \begin{array}{c} p \\ \longrightarrow \\ \bullet \text{---} \bullet \end{array} &= \frac{i(\not{p} + m)}{p^2 - m^2} \\
\text{Spin 1 photon: } \begin{array}{c} p \\ \longrightarrow \\ \bullet \text{---} \bullet \end{array} &= \frac{-ig^{\sigma\nu}}{p^2}
\end{aligned}$$

The vertex factors are finally given as

$$\begin{aligned}
\text{Photon / Spin } \frac{1}{2} \text{ Fermion: } \begin{array}{c} \nearrow \\ \bullet \\ \searrow \end{array} &= -ie\gamma^\sigma \\
\text{Photon / Spin 0 Boson: } \begin{array}{c} p \\ \nearrow \\ \bullet \\ \searrow \\ p' \end{array} &= -iq_H(p + p')^\sigma
\end{aligned}$$

## A.4 Feynman-Parameterization

The Feynman parameterization was developed and first used by Richard Feynman [29] to evaluate loop integrals arising from Feynman diagrams with one or more loops. The most general formula used in this technique is given as

$$\left(\prod_{i=1}^n A_i\right)^{-1} = \int_{[0;1]^n} \prod_{i=1}^n dx_i \delta\left(\sum_{i=1}^n x_i - 1\right) \frac{(n-1)!}{(\sum_{i=1}^n A_i x_i)^n}. \quad (\text{A.4.1})$$

*Proof.* The one-loop integrals to be evaluated in this thesis correspond to the Feynman parameterization for  $n = 3$ . The following calculation verifies eq. (A.4.1) for this case:

$$\begin{aligned} \frac{1}{ABC} &\stackrel{!}{=} \iiint_0^1 dx dy dz \delta(x + y + z - 1) \frac{2}{(Ax + By + Cz)^3} \\ &= \int_0^1 dz \int_0^{1-z} dy \frac{2}{(A + (B-A)y + (C-A)z)^3}. \end{aligned}$$

We can now substitute  $t := A + (B-A)y + (C-A)z$  and obtain

$$\begin{aligned} &\int_0^1 dz \int_0^{1-z} dy \frac{2}{(A + (B-A)y + (C-A)z)^3} \\ &= \frac{2}{B-A} \int_0^1 dz \int_{A+(C-A)z}^{B+(C-B)z} \frac{1}{t^3} dt \\ &= \frac{1}{B-A} \int_0^1 \left( \frac{1}{(A+(C-A)z)^2} - \frac{1}{(B+(C-B)z)^2} \right) dz. \end{aligned}$$

Substituting  $z_1 = (A+(C-A)z)^2$  and  $z_2 = (B+(C-B)z)^2$  yields

$$\begin{aligned} &\frac{1}{B-A} \int_0^1 \left( \frac{1}{(A+(C-A)z)^2} - \frac{1}{(B+(C-B)z)^2} \right) dz \\ &= \frac{1}{B-A} \left( \frac{1}{C-A} \int_A^C \frac{1}{z_1^2} dz_1 - \frac{1}{C-B} \int_B^C \frac{1}{z_2^2} dz_2 \right) \\ &= \frac{1}{B-A} \left( \frac{1}{C-A} \left( \frac{1}{A} - \frac{1}{C} \right) - \frac{1}{C-B} \left( \frac{1}{B} - \frac{1}{C} \right) \right) \\ &= \frac{1}{C(B-A)} \left( \frac{1}{A} - \frac{1}{B} \right) \\ &= \frac{1}{ABC}. \end{aligned}$$

□

The  $\delta$ -distribution enforces that the Feynman parameters sum to one:

$$\sum_i x_i = 1. \quad (\text{A.4.2})$$

## A.5 Contribution to the AMM by the Internal Scalar-Photon interaction

The expression for the amplitude  $\mathcal{M}^\sigma$  is given as

$$\mathcal{M}^\sigma = q_H \int \frac{d^4 q}{(2\pi)^4} \bar{u}(p_2) \frac{(c_s + c_p \gamma^5)(-\not{q} + m_F)(c_s^* - c_p^* \gamma^5)(k_1 + k_2)^\sigma}{(q^2 - m_F^2 + i\varepsilon)(k_2^2 - m_H^2 + i\varepsilon)(k_1^2 - m_H^2 + i\varepsilon)} u(p_1)$$

$$\equiv q_H \int \frac{N^\sigma}{ABC} \frac{d^4q}{(2\pi)^4}. \quad (\text{A.5.1})$$

We can derive the form factor  $F_2(0)$  that contributes to the AMM analogously to Section 3.1. First, the Feynman trick is applied to rewrite the denominator in terms of  $D$ , i.e.

$$\frac{1}{ABC} = 2 \int_0^1 dx dy dz \delta(x+y+z-1) \frac{1}{D^3}, \quad (\text{A.5.2})$$

where  $D$  can be obtained from the Feynman parameterization

$$\begin{aligned} D &= (q^2 - m_F^2 + i\varepsilon)x + (k_2^2 - m_H^2 + i\varepsilon)y + (k_1^2 + m_H^2 + i\varepsilon)z \\ &= q^2 + i\varepsilon - m_F^2 x + p_2^2 y + p_1^2 z - m_H^2(1-x) + 2q_\sigma(p_2^\sigma y + p_1^\sigma z) \\ &= (q^\sigma + p_2^\sigma y + p_1^\sigma z)^2 - (p_2^\sigma y + p_1^\sigma z)^2 - m_F^2 x + (m_\mu^2 - m_H^2)(1-x) + i\varepsilon \\ &\equiv \ell^2 - \Delta + i\varepsilon. \end{aligned} \quad (\text{A.5.3})$$

The momentum shift  $\ell$  and  $\Delta$  are introduced as

$$\ell^\sigma = q^\sigma + p_2^\sigma y + p_1^\sigma z \quad (\text{A.5.4})$$

$$\Delta = m_\mu^2(y^2 + z^2) + 2p_1 p_2 y z + m_F^2 x - (1-x)(m_\mu^2 - m_H^2). \quad (\text{A.5.5})$$

Next, we confront the numerator as follows:

$$\begin{aligned} N^\sigma &= \bar{u} \left\{ (c_s + c_p \gamma^5)(-\not{q} + m_F)(c_s^* - c_p^* \gamma^5)(k_1 + k_2)^\sigma \right\} u \\ &= (c_s + c_p \gamma^5) \underbrace{(-\not{q} + m_F)(2q^\sigma + p_1^\sigma + p_2^\sigma)}_{\xi^\sigma} (c_s^* - c_p^* \gamma^5) \end{aligned} \quad (\text{A.5.6})$$

The inner most part, labeled as  $\xi^\sigma$  can be rearranged by inserting the Feynman parameterization (A.5.4) and (A.5.5):

$$\begin{aligned} \xi^\sigma &= (-\not{\ell} + \not{p}_2 y + \not{p}_1 z + m_F) \cdot 2 \left[ \ell^\sigma - p_2^\sigma (y - \frac{1}{2}) - p_1^\sigma (z - \frac{1}{2}) \right] \\ &= -\frac{1}{2} \ell^2 \gamma^\sigma - 2 (\not{p}_2 y + \not{p}_1 z + m_F) (p_2^\sigma (y - \frac{1}{2}) + p_1^\sigma (z - \frac{1}{2})), \end{aligned} \quad (\text{A.5.7})$$

where the symmetry of the integrand and eq. (2.3.16) was used in the second step. The whole contributing numerator now reads

$$N_{\text{cont}}^\sigma = \bar{u} \left\{ |c_s|^2 \xi^\sigma - |c_p|^2 \gamma^5 \xi^\sigma \gamma^5 - c_s c_p^* \xi^\sigma \gamma^5 + c_s c_p^* \gamma^5 \xi^\sigma \right\} u$$

Next, we have to recall (A.1.4) to simplify the separate terms involving both even and odd number of  $\gamma$ -matrices. This leaves us with

$$\begin{aligned} N_{\text{cont}}^\sigma &= \bar{u} \left\{ |c_s|^2 \left[ -\frac{1}{2} \ell^2 \gamma^\sigma - \underbrace{2(m_\mu(1-x) + m_F)}_{\chi_+} (p_2^\sigma (y - \frac{1}{2}) + p_1^\sigma (z - \frac{1}{2})) \right] - \right. \\ &\quad - |c_p|^2 \left[ \frac{1}{2} \ell^2 \gamma^\sigma + \underbrace{2(m_\mu(1-x) - m_F)}_{\chi_-} (p_2^\sigma (y - \frac{1}{2}) + p_1^\sigma (z - \frac{1}{2})) \right] - \\ &\quad - c_s c_p^* \left[ -\frac{1}{2} \ell^2 \gamma^\sigma - \underbrace{2(m_\mu(y-z) + m_F)}_{\Phi_+} (p_2^\sigma (y - \frac{1}{2}) + p_1^\sigma (z - \frac{1}{2})) \right] \gamma^5 + \\ &\quad \left. + c_s c_p^* \left[ \frac{1}{2} \ell^2 \gamma^\sigma + \underbrace{2(m_\mu(y-z) - m_F)}_{\Phi_-} (p_2^\sigma (y - \frac{1}{2}) + p_1^\sigma (z - \frac{1}{2})) \right] \gamma^5 \right\} u \end{aligned} \quad (\text{A.5.8})$$

To extract the magnetic form factor, we need to apply the Gordon decomposition. This is done by expressing  $p_1^\sigma$  and  $p_2^\sigma$  via  $p_+^\sigma$  and  $p_-^\sigma$  which gives us

$$N^\sigma = \bar{u} \left\{ -\frac{1}{2}\ell^2\gamma^\sigma \left( |c_s|^2 + |c_p|^2 - 2\text{Re}(c_s c_p^*) \gamma^5 \right) - \left[ |c_s|^2 \chi_+ + |c_p|^2 \chi_- + (c_s c_p^* \Phi_+ + c_p c_s^* \Phi_-) \gamma^5 \right] \left( \frac{z-y}{2} p_-^\sigma - \frac{x}{2} p_+^\sigma \right) \right\} u. \quad (\text{A.5.9})$$

Applying the Gordon identity and neglecting all terms that do not contribute to the AMM, i.e. that are not proportional to  $i\sigma^{\sigma\nu} p_{-\nu}$  yields

$$N_{\text{AMM}}^\sigma = \bar{u} \left\{ -(|c_s|^2 \chi_+ + |c_p|^2 \chi_-) \left( \frac{x}{2} i\sigma^{\sigma\nu} p_{-\nu} \right) \right\} u \\ = \bar{u} \left\{ -m_\mu x \left[ |c_s|^2 (1-x + \Omega_F) + |c_p|^2 (1-x - \Omega_F) \right] i\sigma^{\sigma\nu} p_{-\nu} \right\} u. \quad (\text{A.5.10})$$

By comparing this with the general structure of the amplitude  $M^\sigma$  (2.2.6), we obtain

$$q_H \int \frac{N_{\text{AMM}}^\sigma}{ABC} \frac{d^4\ell}{(2\pi)^4} \stackrel{!}{=} (-ie) \bar{u} \left\{ i\sigma^{\sigma\nu} \frac{p_{-\nu}}{2m} F_M(q') \right\} u. \quad (\text{A.5.11})$$

We can now apply the Feynman trick (A.5.7) and rearrange the equation. The form factor  $F_M(q')$  can then be read off in terms of the mass ratios (3.1.26):

$$F_M(q') = -i4m_\mu^2 \frac{q_H}{e} \int \frac{d^4\ell}{(2\pi)^4} \int_0^1 dx dy dz \delta(x+y+z-1) \times \\ \times \frac{x|c_s|^2(1-x+\Omega_F) + x|c_p|^2(1-x-\Omega_F)}{(\ell^2 - \Delta + i\varepsilon)^3} \\ \stackrel{(2.3.25)}{=} -4m_\mu^2 \frac{q_H}{e} \frac{1}{32\pi^2} \int_0^1 dx dy dz \delta(x+y+z-1) \times \\ \times \frac{x|c_s|^2(1-x+\Omega_F) + x|c_p|^2(1-x-\Omega_F)}{m_\mu^2(y^2+z^2) + 2p_1 p_2 yz + m_F^2 x - (1-x)(m_\mu^2 - m_H^2)}. \quad (\text{A.5.12})$$

Evaluating the  $\delta$ -function and taking  $q' = 0$  simplifies the expression above to

$$F_M(0) \stackrel{(2.2.2)}{=} -\frac{q_H}{8\pi^2 e} \int_0^1 dx \int_0^{1-x} dy \frac{x|c_s|^2(1-x+\Omega_F) + x|c_p|^2(1-x-\Omega_F)}{(1-x)^2 + \Omega_F x - (1-x)(1-\Omega_H^2)}, \quad (\text{A.5.13})$$

which can now easily be integrated over  $y$ . Substituting  $(1-x)$  with  $u$  finally yields

$$F_M(0) = [a_\mu]_S = -\frac{q_H}{8\pi^2 e} \int_0^1 du \frac{|c_s|^2(u^3 - u^2 + \Omega_F(u^2 - u)) + |c_p|^2(u^3 - u^2 - \Omega_F(u^2 - u))}{u^2 + \Omega_F^2(1-u) + u(\Omega_H^2 - 1)} \\ = -\frac{q_H}{8\pi^2 e} \int_0^1 du \frac{|c_s|^2(u + \Omega_F) + |c_p|^2(u - \Omega_F)}{u^2 + \Omega_F^2(1-u) + u(\Omega_H^2 - 1)} (u^2 - u). \quad (\text{A.5.14})$$

## A.6 Mass Matrix Scalar Bosons

The most general potential for the 2HDM in the rotated Higgs basis is given by

$$V = m_{11}^2(H_1^\dagger H_1) + m_{22}^2(H_2^\dagger H_2) - m_{12}^2(H_1^\dagger H_2 + \text{h.c.}) + \\ + \frac{\lambda_1}{2}(H_1^\dagger H_1)^2 + \frac{\lambda_2}{2}(H_2^\dagger H_2)^2 + \lambda_3(H_1^\dagger H_1)(H_2^\dagger H_2) + \\ + \lambda_4(H_1^\dagger H_2)(H_2^\dagger H_1) + \left[ \frac{\lambda_5}{2}(H_1^\dagger H_2)^2 + \text{h.c.} \right] + \\ + \left[ (\lambda_6(H_1^\dagger H_1) + (\lambda_7(H_2^\dagger H_2))) H_1^\dagger H_2 + \text{h.c.} \right].$$

To compute the mass matrix for the charged scalars,

$$M_{ij}^2 = \frac{\partial^2 V}{\partial \phi_i \partial \phi_j}, \quad \phi_i \in \{G^\pm, H^\pm\},$$

we first expand the potential by inserting the two Higgs doublets

$$H_1 = \frac{1}{\sqrt{2}} \begin{pmatrix} \sqrt{2} G^+ \\ v + H_1^0 + iG^0 \end{pmatrix}, \quad H_2 = \frac{1}{\sqrt{2}} \begin{pmatrix} \sqrt{2} H^+ \\ H_2^0 + iA^0 \end{pmatrix}.$$

The result is the potential  $V$  as a function of the respective particle fields:

$$\begin{aligned} V = & m_{11}^2 \left\{ G^- G^+ + \frac{1}{2} \left[ (v + H_1^0)^2 + (G^0)^2 \right] \right\} + m_{22}^2 \left\{ H^- H^+ + \frac{1}{2} \left[ (H_2^0)^2 + (A^0)^2 \right] \right\} + \\ & - m_{12}^2 \left\{ G^- H^+ + \frac{1}{2} (v + H_1^0 - iG^0)(H_2^0 + iA^0) \right\} - \\ & + \left\{ H^- G^+ + \frac{1}{2} (H_2^0 - iA^0)(v + H_1^0 + iG^0) \right\} + \\ & + \frac{\lambda_1}{2} \left\{ G^- G^+ + \frac{1}{2} \left[ (v + H_1^0)^2 + (G^0)^2 \right] \right\}^2 + \frac{\lambda_2}{2} \left\{ H^- H^+ + \frac{1}{2} \left[ (H_2^0)^2 + (A^0)^2 \right] \right\}^2 + \\ & + \lambda_3 \left\{ G^- G^+ + \frac{1}{2} \left[ (v + H_1^0)^2 + (G^0)^2 \right] \right\} \left\{ H^- H^+ + \frac{1}{2} \left[ (H_2^0)^2 + (A^0)^2 \right] \right\} + \\ & + \lambda_4 \left\{ G^- H^+ + \frac{1}{2} (v + H_1^0 - iG^0)(H_2^0 + iA^0) \right\} \left\{ H^- G^+ + \frac{1}{2} (H_2^0 - iA^0)(v + H_1^0 + iG^0) \right\} + \\ & + \frac{\lambda_5}{2} \left\{ G^- H^+ + \frac{1}{2} (v + H_1^0 - iG^0)(H_2^0 + iA^0) \right\}^2 + \\ & + \frac{\lambda_5^*}{2} \left\{ H^- G^+ + \frac{1}{2} (H_2^0 - iA^0)(v + H_1^0 + iG^0) \right\}^2 + \\ & + \lambda_6 \left\{ G^- G^+ + \frac{1}{2} \left[ (v + H_1^0)^2 + (G^0)^2 \right] \right\} \left\{ G^- H^+ + \frac{1}{2} (v + H_1^0 - iG^0)(H_2^0 + iA^0) \right\} + \\ & + \lambda_6^* \left\{ H^- G^+ + \frac{1}{2} (H_2^0 - iA^0)(v + H_1^0 + iG^0) \right\} \left\{ G^- G^+ + \frac{1}{2} \left[ (v + H_1^0)^2 + (G^0)^2 \right] \right\} + \\ & + \lambda_7 \left\{ H^- H^+ + \frac{1}{2} \left[ (H_2^0)^2 + (A^0)^2 \right] \right\} \left\{ G^- H^+ + \frac{1}{2} (v + H_1^0 - iG^0)(H_2^0 + iA^0) \right\} + \\ & + \lambda_7^* \left\{ H^- G^+ + \frac{1}{2} (H_2^0 - iA^0)(v + H_1^0 + iG^0) \right\} \left\{ H^- H^+ + \frac{1}{2} \left[ (H_2^0)^2 + (A^0)^2 \right] \right\}. \end{aligned} \tag{A.6.1}$$

The derivatives with respect to the charged particle fields are now quite easily computed:

$$\begin{aligned} \frac{\partial^2 V}{\partial H^- \partial H^+} = & m_{22}^2 + \lambda_2 \left[ 2H^- H^+ + \frac{1}{2} \left( (H_2^0)^2 + (A^0)^2 \right) \right] + \lambda_3 \left[ G^- G^+ + \frac{1}{2} \left( (v + H_1^0)^2 + (G^0)^2 \right) \right] + \\ & + \lambda_4 G^- G^+ + \lambda_7 \left( 2H^+ G^- + \frac{1}{2} (v + H_1^0 - iG^0)(H_2^0 + iA^0) \right) + \\ & + \lambda_7^* \left( 2H^- G^+ + \frac{1}{2} (H_2^0 - iA^0)(v + H_1^0 + iG^0) \right) \\ = & m_{22}^2 + \lambda_3 \frac{v^2}{2} \\ \frac{\partial^2 V}{\partial G^+ \partial G^-} = & m_{11}^2 + \lambda_1 \left[ 2G^- G^+ + \frac{1}{2} \left( (v + H_1^0)^2 + (G^0)^2 \right) \right] + \lambda_3 \left[ H^- H^+ + \frac{1}{2} \left( (H_2^0)^2 + (A^0)^2 \right) \right] + \\ & + \lambda_4 H^+ H^- + \lambda_6 \left[ 2G^- H^+ + \frac{1}{2} (v + H_1^0 - iG^0)(H_2^0 + iA^0) \right] + \\ & + \lambda_6^* \left( 2H^- G^+ + \frac{1}{2} (H_2^0 - iA^0)(v + H_1^0 + iG^0) \right) \\ = & m_{11}^2 + \lambda_1 \frac{v^2}{2} \end{aligned}$$

$$\begin{aligned}
\frac{\partial^2 V}{\partial G^- \partial H^+} &= -m_{12}^2 + \lambda_3 H^- G^+ + \lambda_4 \left( H^- G^+ + \frac{1}{2} (H_2^0 - iA^0)(v + H_1^0 + iG^0) \right) + \\
&\quad + \lambda_5 \left( 2G^- H^+ + \frac{1}{2} (v + H_1^0 - iG^0)(H_2^0 + iA^0) \right) + \\
&\quad + \lambda_6 \left[ 2G^- G^+ + \frac{1}{2} \left( (v + H_2^0)^2 + (G^0)^2 \right) \right] + \\
&\quad + \lambda_7 \left[ 2H^- H^+ + \frac{1}{2} \left( (H_2^0)^2 + (A^0)^2 \right) \right] \\
&= -m_{12}^2 + \lambda_6 \frac{v^2}{2} \\
\frac{\partial^2 V}{\partial G^+ \partial H^-} &= -m_{12}^2 + \lambda_3 G^- H^+ + \lambda_4 \left( G^- H^+ + \frac{1}{2} (v + H_1^0 - iG^0)(H_2^0 + iA^0) \right) + \\
&\quad + \lambda_5^* \left( 2H^- G^+ + \frac{1}{2} (H_2^0 - iA^0)(v + H_1^0 + iG^0) \right) + \\
&\quad + \lambda_6^* \left[ 2G^- G^+ + \frac{1}{2} \left( (v + H_2^0)^2 + (G^0)^2 \right) \right] + \\
&\quad + \lambda_7^* \left[ 2H^- H^+ + \frac{1}{2} \left( (H_2^0)^2 + (A^0)^2 \right) \right] \\
&= -m_{12}^2 + \lambda_6 \frac{v^2}{2}
\end{aligned}$$

The derivatives were respectively simplified by neglecting all the coupling terms in the potential that do not include mass contributions. The minimization conditions for the potential can be derived by performing the first order derivatives with respect to the distinct Higgs fields, which leads to

$$\begin{aligned}
\left( \frac{\partial V}{\partial H_1} \right) &= 0 & \left( \frac{\partial V}{\partial H_2} \right) &= 0 \\
\Rightarrow m_{11}^2 &= -\lambda_1 \frac{v^2}{2} & \Rightarrow m_{12}^2 &= \lambda_6 \frac{v^2}{2}
\end{aligned} \tag{A.6.2} \tag{A.6.3}$$

They can now finally get inserted into the matrix elements which can be combined to form the mass matrix given in Section 4.1:

$$M_{\text{charged}}^2 = \begin{pmatrix} m_{22}^2 + \frac{1}{2} v^2 \lambda_3 & 0 \\ 0 & 0 \end{pmatrix}. \tag{A.6.4}$$

## A.7 Projection operators

Section 2.1 introduces the four component Dirac spinor  $\psi = (\psi_A \ \psi_B)^T$ . It turns out that  $\psi_A \equiv \psi_L$  and  $\psi_B \equiv \psi_R$  are the left- and right-handed Weyl spinors which refer to the  $(\frac{1}{2}, 0)$  and  $(0, \frac{1}{2})$  representation of the Lorentz group. These spinors are eigenstates of the so-called chirality operator in Weyl representation

$$\gamma^5 = \begin{pmatrix} -\mathbb{1} & 0 \\ 0 & \mathbb{1} \end{pmatrix} \tag{A.7.1}$$

with eigenvalues  $\mp 1$  and thus represent massless particles (like neutrinos) with left- and right-handed chirality. We can now define the left- and right-handed projection operators

$$P_L = \frac{\mathbb{1} - \gamma^5}{2} = \begin{pmatrix} 1 & 0 \\ 0 & 0 \end{pmatrix} \quad \text{and} \quad P_R = \frac{\mathbb{1} + \gamma^5}{2} = \begin{pmatrix} 0 & 0 \\ 0 & 1 \end{pmatrix} \tag{A.7.2}$$

which when acting on the Dirac spinor  $\psi$  pick out the left- and right-handed Weyl spinor, respectively.

# Bibliography

- [1] Kai Schmidt-Hoberg. “Phenomenology of Physics beyond the Standard Model”. In: (May 27, 2015), p. 80. URL: [https://www.desy.de/~kschmidt/BSM\\_lecturenotes.pdf](https://www.desy.de/~kschmidt/BSM_lecturenotes.pdf) (visited on 08/20/2025).
- [2] Julian Schwinger. “Quantum Electrodynamics. III. The Electromagnetic Properties of the Electron Radiative Corrections to Scattering”. In: *Physical Review* 76.6 (Sept. 15, 1949), pp. 790–817. ISSN: 0031-899X. DOI: [10.1103/PhysRev.76.790](https://doi.org/10.1103/PhysRev.76.790). URL: <https://link.aps.org/doi/10.1103/PhysRev.76.790> (visited on 08/19/2025).
- [3] Tatsumi Aoyama et al. “Complete Tenth-Order QED Contribution to the Muon  $g-2$ ”. In: *Physical Review Letters* 109.11 (Sept. 13, 2012). Publisher: American Physical Society, p. 111808. DOI: [10.1103/PhysRevLett.109.111808](https://doi.org/10.1103/PhysRevLett.109.111808). URL: <https://link.aps.org/doi/10.1103/PhysRevLett.109.111808> (visited on 08/20/2025).
- [4] The Muon  $g-2$  Collaboration et al. *Measurement of the Positive Muon Anomalous Magnetic Moment to 127 ppb*. June 3, 2025. DOI: [10.48550/arXiv.2506.03069](https://doi.org/10.48550/arXiv.2506.03069). arXiv: [2506.03069](https://arxiv.org/abs/2506.03069) [hep-ex]. URL: <http://arxiv.org/abs/2506.03069> (visited on 08/07/2025).
- [5] F. Halzen and A.D. Martin. *Quarks & Leptons*. New York, USA: John Wiley & Sons, 1984.
- [6] Friedrich Jegerlehner. *The Anomalous Magnetic Moment of the Muon*. Vol. 274. Springer Tracts in Modern Physics. Cham: Springer International Publishing, 2017. ISBN: 978-3-319-63575-0 978-3-319-63577-4. DOI: [10.1007/978-3-319-63577-4](https://doi.org/10.1007/978-3-319-63577-4). URL: <http://link.springer.com/10.1007/978-3-319-63577-4> (visited on 08/07/2025).
- [7] Michael Edward Peskin and Daniel V. Schroeder. *An introduction to quantum field theory*. The advanced book program. Boca Raton London New York: CRC Press, Taylor & Francis Group, 2019. 842 pp. ISBN: 978-0-201-50397-5 978-0-367-32056-0.
- [8] Jacques P. Leveille. “The second-order weak correction to  $(g - 2)$  of the muon in arbitrary gauge models”. In: *Nuclear Physics B* 137.1 (May 1978), pp. 63–76. ISSN: 05503213. DOI: [10.1016/0550-3213\(78\)90051-2](https://doi.org/10.1016/0550-3213(78)90051-2). URL: <https://linkinghub.elsevier.com/retrieve/pii/0550321378900512> (visited on 08/07/2025).
- [9] Lei Wang, Jin Min Yang, and Yang Zhang. “Two-Higgs-doublet models in light of current experiments: a brief review”. In: *Communications in Theoretical Physics* 74.9 (Sept. 1, 2022), p. 097202. ISSN: 0253-6102, 1572-9494. DOI: [10.1088/1572-9494/ac7fe9](https://doi.org/10.1088/1572-9494/ac7fe9). arXiv: [2203.07244](https://arxiv.org/abs/2203.07244) [hep-ph]. URL: <http://arxiv.org/abs/2203.07244> (visited on 08/07/2025).
- [10] Sudip Jana, Vishnu P. K, and Shaikh Saad. “Resolving electron and muon  $g-2$  within the 2HDM”. In: *Physical Review D* 101.11 (June 29, 2020), p. 115037. ISSN: 2470-0010, 2470-0029. DOI: [10.1103/PhysRevD.101.115037](https://doi.org/10.1103/PhysRevD.101.115037). arXiv: [2003.03386](https://arxiv.org/abs/2003.03386) [hep-ph]. URL: <http://arxiv.org/abs/2003.03386> (visited on 08/07/2025).
- [11] Yue-Liang Wu and Lincoln Wolfenstein. “Sources of CP Violation in the Two-Higgs Doublet Model”. In: *Physical Review Letters* 73.13 (Sept. 26, 1994), p. 2. DOI: [10.1103/PhysRevLett.73.1762](https://doi.org/10.1103/PhysRevLett.73.1762). arXiv: [hep-ph/9409421](https://arxiv.org/abs/hep-ph/9409421). URL: <https://doi.org/10.48550/arXiv.hep-ph/9409421> (visited on 08/07/2025).

- [12] ATLAS Collaboration. “Search for charged Higgs bosons decaying via  $H^+ \rightarrow \tau \nu$  in top quark pair events using pp collision data at  $\sqrt{s} = 7$  TeV with the ATLAS detector”. In: *Journal of High Energy Physics* 2012.6 (June 2012), 39, JHEP06(2012)039. ISSN: 1029-8479. DOI: [10.1007/JHEP06\(2012\)039](https://doi.org/10.1007/JHEP06(2012)039). arXiv: [1204.2760](https://arxiv.org/abs/1204.2760). URL: <http://arxiv.org/abs/1204.2760> (visited on 08/07/2025).
- [13] K. S. Babu and Sudip Jana. “Enhanced Di-Higgs Production in the Two Higgs Doublet Model”. In: *Journal of High Energy Physics* 2019.2 (Feb. 2019), p. 193. ISSN: 1029-8479. DOI: [10.1007/JHEP02\(2019\)193](https://doi.org/10.1007/JHEP02(2019)193). arXiv: [1812.11943v2](https://arxiv.org/abs/1812.11943v2). URL: <http://arxiv.org/abs/1812.11943> (visited on 08/07/2025).
- [14] K. S. Babu, Sudip Jana, and Vishnu P. K. “Correlating  $W$ -Boson Mass Shift with Muon  $g-2$  in the 2HDM”. In: *Physical Review Letters* 129.12 (Sept. 14, 2022), p. 121803. ISSN: 0031-9007, 1079-7114. DOI: [10.1103/PhysRevLett.129.121803](https://doi.org/10.1103/PhysRevLett.129.121803). arXiv: [2204.05303](https://arxiv.org/abs/2204.05303). URL: <http://arxiv.org/abs/2204.05303> (visited on 08/08/2025).
- [15] Babette Döbrich et al. “ALPtraum: ALP production in proton beam dump experiments”. In: *Journal of High Energy Physics* 2016.2 (Feb. 2, 2016), p. 18. ISSN: 1029-8479. DOI: [10.1007/JHEP02\(2016\)018](https://doi.org/10.1007/JHEP02(2016)018). URL: [https://doi.org/10.1007/JHEP02\(2016\)018](https://doi.org/10.1007/JHEP02(2016)018) (visited on 08/22/2025).
- [16] Matthew J. Dolan et al. “Revised constraints and Belle II sensitivity for visible and invisible axion-like particles”. In: *Journal of High Energy Physics* 2017.12 (Dec. 18, 2017), p. 94. ISSN: 1029-8479. DOI: [10.1007/JHEP12\(2017\)094](https://doi.org/10.1007/JHEP12(2017)094). URL: [https://doi.org/10.1007/JHEP12\(2017\)094](https://doi.org/10.1007/JHEP12(2017)094) (visited on 08/22/2025).
- [17] J. D. Bjorken et al. “Search for neutral metastable penetrating particles produced in the SLAC beam dump”. In: *Physical Review D* 38.11 (Dec. 1, 1988). Publisher: American Physical Society, pp. 3375–3386. DOI: [10.1103/PhysRevD.38.3375](https://doi.org/10.1103/PhysRevD.38.3375). URL: <https://link.aps.org/doi/10.1103/PhysRevD.38.3375> (visited on 08/14/2025).
- [18] J. P. Lees et al. “Search for a muonic dark force at BaBar”. In: *Physical Review D* 94.1 (July 19, 2016). Publisher: American Physical Society, p. 011102. DOI: [10.1103/PhysRevD.94.011102](https://doi.org/10.1103/PhysRevD.94.011102). URL: <https://link.aps.org/doi/10.1103/PhysRevD.94.011102> (visited on 08/14/2025).
- [19] A. M. Sirunyan et al. “Search for an  $L\bar{t} - L$  gauge boson using  $Z4\bar{t}$  events in proton-proton collisions at  $\sqrt{s}=13$ TeV”. In: *Physics Letters B* 792 (May 10, 2019), pp. 345–368. ISSN: 0370-2693. DOI: [10.1016/j.physletb.2019.01.072](https://doi.org/10.1016/j.physletb.2019.01.072). URL: <https://www.sciencedirect.com/science/article/pii/S037026931930214X> (visited on 08/15/2025).
- [20] T. Abe et al. *Belle II Technical Design Report*. Nov. 1, 2010. DOI: [10.48550/arXiv.1011.0352](https://doi.org/10.48550/arXiv.1011.0352). arXiv: [1011.0352\[physics\]](https://arxiv.org/abs/1011.0352). URL: <http://arxiv.org/abs/1011.0352> (visited on 08/15/2025).
- [21] Brian Batell et al. “Flavor-specific scalar mediators”. In: *Physical Review D* 98.5 (Sept. 20, 2018), p. 055026. ISSN: 2470-0010, 2470-0029. DOI: [10.1103/PhysRevD.98.055026](https://doi.org/10.1103/PhysRevD.98.055026). URL: <https://link.aps.org/doi/10.1103/PhysRevD.98.055026> (visited on 08/15/2025).
- [22] H. Albrecht et al. “A search for the lepton-flavour violating decays  $e, \mu \rightarrow \nu e, \nu \mu$ ”. In: *Zeitschrift für Physik C Particles and Fields* 68.1 (Mar. 1, 1995), pp. 25–28. ISSN: 1431-5858. DOI: [10.1007/BF01579801](https://doi.org/10.1007/BF01579801). URL: <https://doi.org/10.1007/BF01579801> (visited on 08/14/2025).
- [23] Rahool Kumar Barman, Ritu Dcruz, and Anil Thapa. “Neutrino masses and magnetic moments of electron and muon in the Zee Model”. In: *Journal of High Energy Physics* 2022.3 (Mar. 28, 2022), p. 183. ISSN: 1029-8479. DOI: [10.1007/JHEP03\(2022\)183](https://doi.org/10.1007/JHEP03(2022)183). URL: [https://doi.org/10.1007/JHEP03\(2022\)183](https://doi.org/10.1007/JHEP03(2022)183) (visited on 08/14/2025).

- 
- [24] A. Hayrapetyan et al. “Search for the lepton-flavor violating decay of the Higgs boson and additional Higgs bosons in the  $e^-$  final state in proton-proton collisions at  $\sqrt{s} = 13$  TeV”. In: *Physical Review D* 108.7 (Oct. 10, 2023), p. 072004. ISSN: 2470-0010, 2470-0029. DOI: [10.1103/PhysRevD.108.072004](https://doi.org/10.1103/PhysRevD.108.072004). URL: <https://link.aps.org/doi/10.1103/PhysRevD.108.072004> (visited on 08/14/2025).
- [25] S. Chatrchyan et al. “Observation of Z decays to four leptons with the CMS detector at the LHC”. In: *Journal of High Energy Physics* 2012.12 (Dec. 7, 2012), p. 34. ISSN: 1029-8479. DOI: [10.1007/JHEP12\(2012\)034](https://doi.org/10.1007/JHEP12(2012)034). URL: [https://doi.org/10.1007/JHEP12\(2012\)034](https://doi.org/10.1007/JHEP12(2012)034) (visited on 08/14/2025).
- [26] Iftah Galon, Anna Kwa, and Philip Tanedo. “Lepton-Flavor Violating Mediators”. In: *Journal of High Energy Physics* 2017.3 (Mar. 2017), p. 64. ISSN: 1029-8479. DOI: [10.1007/JHEP03\(2017\)064](https://doi.org/10.1007/JHEP03(2017)064). arXiv: [1610.08060 \[hep-ph\]](https://arxiv.org/abs/1610.08060). URL: <http://arxiv.org/abs/1610.08060> (visited on 08/26/2025).
- [27] S. Navas et al. *e*. Particle Data Group. May 30, 2025. URL: [https://pdg.lbl.gov/2025/listings/contents\\_listings.html](https://pdg.lbl.gov/2025/listings/contents_listings.html) (visited on 08/26/2025).
- [28] Yoav Afik, P. S. Bhupal Dev, and Anil Thapa. “Hints of a new leptophilic Higgs sector?”. In: *Physical Review D* 109.1 (Jan. 2, 2024), p. 015003. ISSN: 2470-0010, 2470-0029. DOI: [10.1103/PhysRevD.109.015003](https://doi.org/10.1103/PhysRevD.109.015003). URL: <https://link.aps.org/doi/10.1103/PhysRevD.109.015003> (visited on 08/14/2025).
- [29] R. P. Feynman. “Space-Time Approach to Quantum Electrodynamics”. In: *Physical Review* 76.6 (Sept. 15, 1949), pp. 769–789. ISSN: 0031-899X. DOI: [10.1103/PhysRev.76.769](https://doi.org/10.1103/PhysRev.76.769). URL: <https://link.aps.org/doi/10.1103/PhysRev.76.769> (visited on 08/19/2025).